Inorganic Chemistry

pubs.acs.org/IC

Article

Mixed-Isocyanide Complexes of Technetium under Steric and Electronic Control

Guilhem Claude, Jonas Genz, Dominik Weh, Maximilian Roca Jungfer, Adelheid Hagenbach, Milan Gembicky, Joshua S. Figueroa,* and Ulrich Abram*

Cite This: *Inorg. Chem.* 2022, 61, 16163−16176

Read Online

ACCESS | Metrics & More | Article Recommendations | Supporting Information

ABSTRACT: Reactions of the alkyl isocyanide *fac*-[Tc(CO)$_3$(CNR)$_2$Cl] complexes (**2**) (CNR = CN^{n}Bu or CN^{t}Bu) with the sterically encumbered isocyanide CN*p*-FAr^{DarF2} [DArF = 3,5-(CF$_3$)$_2$C$_6$H$_3$] allow a selective exchange of the carbonyl ligands of **2** and the isolation of the mixed-isocyanide complexes *mer,trans*-[Tc(CN*p*-FAr^{DarF2})$_3$(CNR)$_2$Cl] (**3**). Depending on the steric requirements of the residues *R*, the remaining chlorido ligand can be replaced by another isocyanide ligand. Cationic complexes such as *mer*-[Tc(CN*p*-FAr^{DarF2})$_3$(CN^{n}Bu)$_3$]$^+$ (**4a**) or *mer,trans*-[Tc(CN*p*-FAr^{DarF2})$_3$(CN^{n}Bu)$_2$(CN^{t}Bu)]$^+$ (**6**) have been prepared in this way and isolated as their PF_6^- salts. *mer,trans*-[Tc(CN*p*-FAr^{DarF2})$_3$(CN^{n}Bu)$_2$(CN^{t}Bu)](PF$_6$) represents to the best of our knowledge the first transition-metal complex with three different isocyanides in its coordination sphere. Since the degree of the ligand exchange seems to be controlled both by the electronic and steric measures of the incoming isocyanides, we undertook similar reactions with the sterically less demanding *p*-fluorophenyl isocyanide, CNPh^{pF}, which indeed readily led to the hexakis(isocyanide)technetium(I) cation through an exchange of all ligands in the staring materials [Tc$_2$(CO)$_6$(*μ*-Cl)$_3$]$^-$ or *fac*-[Tc(CO)$_3$(CNR)$_2$Cl]. The influence of the substituents at the isocyanide ligands in such reactions has been reasoned with the density functional theory-derived electrostatic potential at the accessible surface of the corresponding isocyanide carbon atoms.

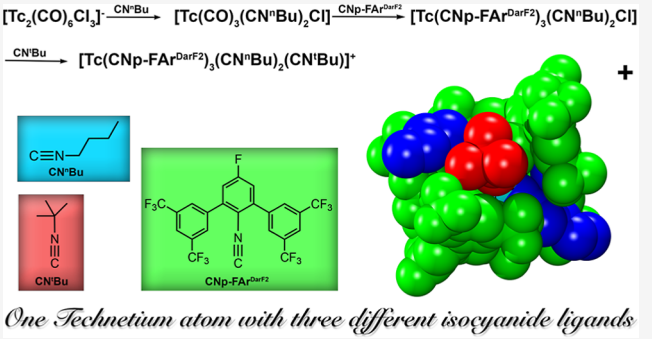

INTRODUCTION

The chemistry of technetium isocyanides is dominated by the tremendous success story of ^{99m}Tc-Sestamibi (Cardiolite), which has been used by more than 40 million patients for myocardial imaging.[1] ^{99m}Tc-Sestamibi is a hexakis(isocyanide)-technetium(I) cation with 2-methoxy-2-methylpropylisonitrile (MIBI, see Chart 1). The clinically relevant kit formulation using the metastable nuclear isomer ^{99m}Tc (pure gamma emitter, half-life: 6.01 h) produces the technetium(I) cation at a nanomolar scale directly from $^{99m}TcO_4^-$ with $SnCl_2$ as a reductant. The isocyanide is provided by a transmetallation reaction starting from the [Cu(MIBI)$_4$]$^+$ cation.[2] For chemical studies with the long-lived isotope ^{99}Tc (weak beta emitter, half-life: 2.11 × 10^5 a), a reductive ligand-exchange procedure starting from the technetium(III) complex [Tc(tu)$_6$]$^{3+}$ (tu = thiourea) is the preferred synthesis and a considerable number of hexakis(isocyanide)technetium(I) complexes have been prepared by this approach or directly from pertechnetate via a reduction with sodium dithionite.[3−8] The resulting [Tc(CNR)$_6$]$^+$ cations (R = alkyl, aryl) have a d^6 configuration and are relatively inert against attempted ligand exchange reactions. A considerable reactivity is only observed under harsh conditions.[9−11]

In contrast to technetium(I) hexakis(isonitrile) complexes, the chemistry of other technetium complexes with isocyanide ligands is little explored. There are some systematic studies about technetium(III) and -(IV) complexes with isocyanides and "umbrella-like" tri- and tetradentate chelators, which also found consideration for nuclear medical labeling procedures.[12−19] Additionally, isocyanides have been used as co-ligands in low-valent technetium complexes with phosphines and imines.[20−27]

Compounds of particular interest are carbonyl complexes with isocyanide co-ligands. Alkyl and aryl isocyanides are isoelectronic and frequently regarded as structural and electronic surrogates for carbonyl ligands but with a stronger tendency to act as a *σ*-donor and with a weaker *π*-acceptor character. However, such a general description is merely a rough approximation since, particularly, the *π*-acceptor

Received: July 30, 2022
Published: September 27, 2022

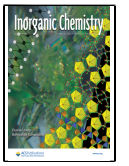

https://doi.org/10.1021/acs.inorgchem.2c02730
Inorg. Chem. 2022, 61, 16163−16176

Chart 1. Isocyanide Ligands and Their Abbreviations Mentioned in the Present Paper

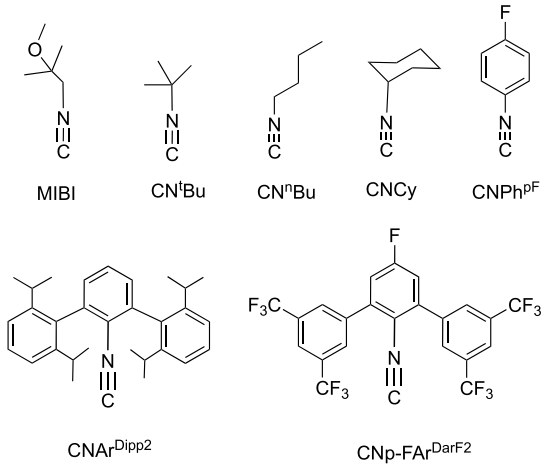

behavior is strongly influenced by the substituents R of the C≡N−R ligands. Additionally, steric effects and the formal oxidation state of the metal ion significantly influence the resulting M−C bond strengths in carbonyl and isocyanide complexes. Although the ready replacement of CO by isocyanide ligands is documented for several metals including a limited number of reactions with manganese and rhenium carbonyls,[28,29] such reactions are rare for technetium. The synthesis of pentacarbonyltechnetium(I) complexes with one additional isocyanide ligand can readily be performed by a selective exchange of a halide from $[Tc(CO)_5X]$ species (X = Cl, Br, I). Such reactions are commonly conducted under mild conditions and with the addition of Ag^+ ions as halide scavengers,[30,31] while heating of the pentacarbonyl halides with an excess of isocyanides results in the formation of neutral tricarbonyl compounds of the composition *fac*-$[Tc(CO)_3X(CNR)_2]$.[32,33]

Such facial tricarbonyltechnetium(I) complexes are also obtained during reactions of $(NEt_4)_2[Tc(CO)_3Cl_3]$ or $(NBu_4)[Tc_2(CO)_6(\mu\text{-}Cl)_3]$ (Scheme 1) with alkyl isocyanides.[34−36] Corresponding procedures for the short-lived nuclide ^{99m}Tc have been developed and alkyl and aryl isocyanides have been used as components in mixed-ligand complexes having the *fac*-$\{Tc(CO)_3\}^+$ core.[37−39] The replacement of the halide ligand from *fac*-$[Tc(CO)_3X(CNR)_2]$ by a third isocyanide is solvent-dependent and has been reported to occur slowly in water. Reactions in organic solvents are less efficient and do not yield pure products with satisfactory yields.[40] Heating and the related ongoing decomposition of the isocyanides can be avoided by the addition of Ag^+ ions, which results in the precipitation of AgCl and salts of the *fac*-$[Tc(CO)_3(CN^tBu)_3]^+$ cation have been isolated in good yields.[36,40] Hitherto, no ongoing replacement of carbonyl ligands has been observed. The same holds true for reactions of $(NBu_4)[Tc_2(CO)_6(\mu\text{-}Cl)_3]$ with the sterically demanding isocyanide CNAr^{Dipp2} (Dipp = 2,6-diisopropylphenyl) (see Chart 1), where a ligand rearrangement is found and finally *trans,mer*-$[Tc(CO)_3Cl(CNAr^{Dipp2})_2]$ is formed.[41] The observed isomerization of the *fac*-$\{Tc(CO)_3\}^+$ core into the thermodynamically less favored meridional configuration can be understood by the steric demand of the CNAr^{Dipp2} ligands. Similar observations have been made for other transition-metal carbonyls.[42−45] Thus, it was surprising that during reactions of

Scheme 1. Synthesis and Reactions of Carbonyltechnetium Complexes with Isocyanide Ligands

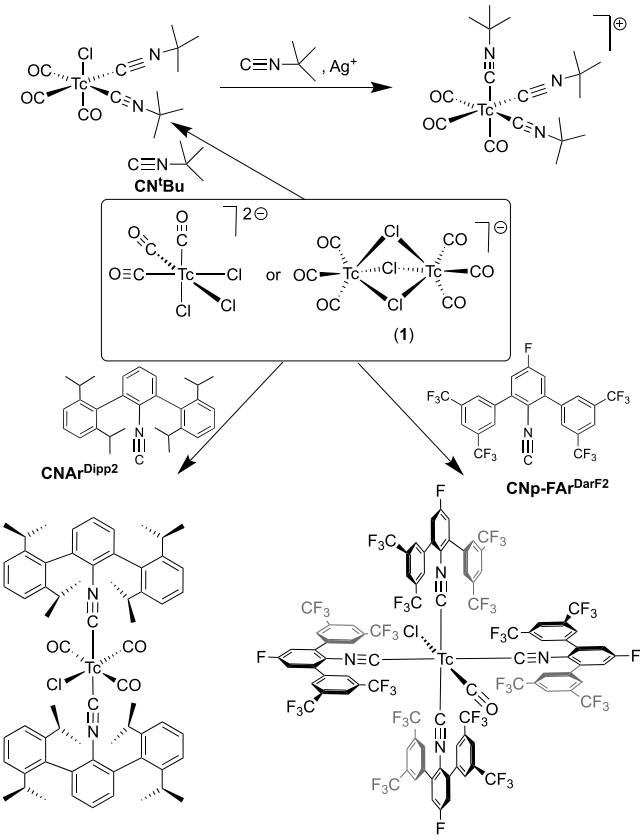

$(NBu_4)[Tc_2(CO)_6(\mu\text{-}Cl)_3]$ with the fluorine-substituted terphenyl isocyanide CN*p*-FAr^{DarF2} (Chart 1) an ongoing carbonyl exchange was observed, which finally gave the monocarbonyl complex *trans*-$[Tc(CO)Cl(CNp\text{-}FAr^{DarF2})_4]$ with four of the bulky isocyanides in equatorial positions (Scheme 1).[46] Similar products have also been isolated for rhenium. They form a convenient platform for the synthesis of complexes of group 7 metals in their very low formal oxidation states.[46] On the other hand, the observed ability of CN*p*-FAr^{DarF2} for a selective removal/replacement of carbonyls from the coordination sphere of technetium by this unique ligand stimulated us to explore the synthetic potential of this behavior for the synthesis of novel low-valent technetium complexes but also the reasons for the observed unusual reactivity.

Here, we present a stepwise synthetic approach to unprecedented, well-defined technetium complexes with different isocyanides in their coordination sphere and a novel access to hexakis(isocyanide)technetium(I) cations starting from the common precursor $(NBu_4)[Tc_2(CO)_6(\mu\text{-}Cl)_3]$.

EXPERIMENTAL SECTION

General Considerations. Unless otherwise stated, reagent-grade starting materials were purchased from commercial sources and either used as received or purified by standard procedures. Solvents were dried and deoxygenated according to standard procedures. $(NBu_4)[Tc_2(CO)_6(\mu\text{-}Cl)_3]$ (**1**) was prepared by a literature procedure.[36] The syntheses of CN*p*-FAr^{DarF2} and CNPh^{pF} were done by modified literature procedures.[47,48]

Physical Measurements. NMR spectra were recorded using JEOL 400 MHz ECS or ECZ multinuclear spectrometers. The values given for the ^{99}Tc chemical shifts are referenced to potassium pertechnetate in water. IR spectra were recorded using a Shimadzu

https://doi.org/10.1021/acs.inorgchem.2c02730
Inorg. Chem. 2022, 61, 16163−16176

FTIR 8300 spectrometer as KBr pellets (Tc complexes) or an FT IR spectrometer (Nicolet iS10, Thermo Scientific) (organic compounds). Intensities are classified as vs = very strong, s = strong, m = medium, w = weak, vw = very weak, sh = shoulder. The following abbreviations were used for the intensities and characteristics of IR absorption bands: vs = very strong, s = strong, m = medium, w = weak, sh = shoulder.

Radiation Precautions. ^{99}Tc is a long-lived, weak β^- emitter (E_{max} = 0.292 MeV). Normal glassware provides adequate protection against weak beta radiation when milligram amounts are used. Secondary X-rays (bremsstrahlung) play a significant role only when larger amounts of ^{99}Tc are handled. All manipulations were done in a laboratory approved for the handling of radioactive materials.

X-ray Crystallography. The intensities for the X-ray determinations were collected on STOE IPDS II or on Bruker D8 Venture instruments with Mo Kα radiation. The space groups were determined by the detection of systematical absences. Absorption corrections were carried out by multiscan or integration methods.[49,50] Structure solution and refinement were performed using the SHELX program package.[51,52] Hydrogen atoms were derived from the final Fourier maps and refined or placed at calculated positions and treated with the "riding model" option of SHELXL. The representation of molecular structures was done using the program DIAMOND 4.2.2.[53]

Additional information on the structure determinations is contained in the Supporting Information and has been deposited with the Cambridge Crystallographic Data Centre.

Computational Details. Density functional theory (DFT) calculations were performed on the high-performance computing systems of the Freie Universität Berlin ZEDAT (Curta)[54] using the program package Gaussian 16.[55] Gas-phase geometry optimizations were performed using initial coordinates generated using GaussView and Avogadro.[56,57] The calculations were performed using the hybrid density functional B3LYP.[58−60] Br and I atoms were modeled using the 6-311G** basis functions.[61,62] The 6-311++G** basis set was used to model all remaining elements.[63−67] All basis sets as well as the electrochemical potentials (ECPs) were obtained from the EMSL database.[68] Frequency calculations after the optimizations confirmed the convergence. No negative frequencies were obtained for the given optimized geometries of all compounds. The surface properties module of the multifunctional wave-function analyzer MultiWFN was used for the calculation of the surface properties.[69]

Syntheses. *CNp-FAr^{DarF2}.* The isocyanide was synthesized using a modified literature procedure.[48] Solvents were not dried prior to use. Na_2CO_3 (4.93 g), 2,6-dibromo-4-fluoroaniline (2.85 g, 11.5 mmol), and (3,5-bis(trifluoromethyl)phenyl)boronic acid (6.00 g, 23 mmol) were added to degassed toluene (90 mL) in a 350 mL pressure vessel. In a separate flask, tris(dibenzylidenaceton)dipalladium(0) (99 mg) in degassed toluene (30 mL) was treated with triphenylphosphine (57 mg). The solution was stirred until the color changed from red to orange and was then transferred to the pressure vessel. Degassed water (15 mL) and degassed ethanol (30 mL) were added to the solution. The pressure vessel was then closed tightly and kept at 90 °C for 2 days. After cooling to room temperature, brine (30 mL) was added, and the pH was adjusted to 7 using 0.1 M HCl. The phases were separated, and the aqueous layer was extracted with Et_2O (3 × 15 mL). The combined organic phases were dried over Na_2SO_4, and volatiles were removed under vacuum. The crude product was loaded onto silica with CH_2Cl_2 and purified by column chromatography (*n*-hexane/CH_2Cl_2 3.75:1). Volatiles were removed under vacuum and the corresponding amine, H_2N(*p*-Far^{DarF2}), was obtained as a colorless solid. Yield: 5.35 g, 9.99 mmol, 87%.

A solution of the thus-prepared H_2N(*p*-FAr^{DArF2}) in toluene (20 mL) was added to a solution of formic acid, which was prepared by heating a mixture of acetic anhydride (30 mL) and formyl acetamide (19 mL) at 70 °C. The mixture was kept at 70 °C for 30 min and the progress of the reaction was monitored by ^{19}F NMR. Once the ^{19}F NMR spectra indicated full conversion, volatiles were entirely removed under reduced pressure at 50 °C (Caution! the volatiles are corrosive) to give HC(O)NH^{DArF} of sufficient purity for the dehydration reaction. The complete removal of the acidic volatiles is the prerequisite for the last step. The crude HC(O)NH^{DArF} was dissolved in dichloromethane (50 mL) and treated with triethylamine (6.3 mL, 45 mmol). The solution was cooled to 0 °C, and phosphoryl chloride (1.3 mL, 13.5 mmol) was slowly added. The progress of the reaction was monitored by ^{19}F NMR spectroscopy after warming to room temperature (approximately 10 min until full conversion). After complete consumption of the amide, a saturated solution of $NaHCO_3$ was slowly added, and the mixture was very vigorously stirred for a few minutes. The phases were separated. The aqueous phase was extracted with dichloromethane (2 × 30 mL), and the unified organic phases were dried over Na_2SO_4. (Note! The use of $MgSO_4$ should be avoided here as its use reduces the yield.) Volatiles were removed under reduced pressure, and the crude product was recrystallized from hot hexane, filtered, washed with a small amount of cold hexane, and dried under reduced pressure. CN*p*-FAr^{DarF2} was obtained as a colorless crystalline solid. Overall yield: 4.35 g, 7.98 mmol, 80%. The analytical data were identical to those reported in the literature.[48]

*fac-[Tc(CO)$_3$(CNR)$_2$Cl] (CNR = CN^{n}Bu: **2a**, CN^{t}Bu: **2b**).* $(NBu_4)[Tc_2(CO)_6(\mu\text{-}Cl)_3]$ (**1**) (36 mg, 0.05 mmol) and the corresponding isocyanide (0.96 mmol) were dissolved in CH_2Cl_2 (5 mL) and heated on reflux for 1.5 h. Volatiles were removed under reduced pressure. The residue was extracted with Et_2O (4 × 5 mL), and the extracts were filtered. Volatiles were then removed under dynamic vacuum for 2 h. **2a**: Colorless oil. Yield: 13 mg (0.03 mmol, 33%) IR (KBr, cm^{-1}): 3397 (br), 2920 (s), 2860 (sh), 2372 (m), 2208 (m, $\nu_{C\equiv N}$), 2046 (s, $\nu_{C\equiv O}$), 1985 (s, $\nu_{C\equiv O}$), 1935 (s, $\nu_{C\equiv O}$), 1466 (m), 1107 (s). ^{1}H NMR ($CDCl_3$, ppm): 3.69 (2H, t, *J* = 6.8 Hz, CH_2), 1.78 (2H, p, *J* = 7.0 Hz, CH_2), 1.50 (2 H, m, *J* = 7.4 Hz, CH_2), 0.98 (3H, t, *J* = 7.4 Hz, CH_3). ^{99}Tc NMR ($CDCl_3$, ppm): −1657 (s, $\nu_{1/2}$ = 2250 Hz). **2b**: Colorless solid. Yield: 12 mg (0.031 mmol, 31%). ^{1}H NMR and IR data are as reported earlier.[34] ^{99}Tc NMR (CD_2Cl_2, ppm): −1654 (s, $\nu_{1/2}$ = 2320 Hz).

*mer,trans-[Tc(CNp-FAr^{DarF2})$_3$(CNR)$_2$Cl] (CNR = CN^{n}Bu: **3a**, CN^{t}Bu: **3b**).* $[Tc(CNR)_2(CO)_3Cl]$ (0.05 mmol) was dissolved in toluene (5 mL). CN*p*-FAr^{DarF2} (219 mg, 0.40 mmol) was added, and the solution was heated on reflux for 6 h. The color of the solution turned deep orange−yellow. The progress of the reaction was monitored via ^{99}Tc NMR spectroscopy. The solvent was removed under reduced pressure, and the residue was extracted with diethyl ether. The orange−red extracts were filtered, and the remaining solid was washed with diethyl ether (5 mL). *n*-Hexane (2 mL) was added, and the solution was concentrated slowly. Orange−yellow single crystals of compound **3b** were obtained directly from this solution. **3b**: Yield: 35 mg (0.018 mmol, 36%.) IR (KBr, cm^{-1}): 2988 (w), 2926 (w), 2114 (s, $\nu_{C\equiv N}$), 2031 (vs, $\nu_{C\equiv N}$), 1925 (s, $\nu_{C\equiv N}$), 1597 (m), 1464(m), 1420 (m), 1396 (m), 1364 (s), 1281 (s), 1171 (s), 1138 (s), 899 (m), 847 (m), 706 (m), 683 (m), 637 (w), 555 (m). ^{1}H NMR (CD_2Cl_2, ppm): 7.91−7.55 (18H, m, aryl-H), 7.07 (6H, m, aryl-H), 0.82 (18H, s, CH_3). ^{19}F NMR (CD_2Cl_2, ppm): −63.7 (12F, s, CF_3), −63.9 (24F, s, CF_3), −111.9 (2F, s, *p*-F),-116.93 (1F, s, *p*-F). ^{99}Tc NMR (CD_2Cl_2, ppm): −1452 (s, $\nu_{1/2} \approx$ 16 kHz). Compound **3a** was not isolated in a crystalline form but directly used for the synthesis of **4a**.

*mer-[Tc(CNp-FAr^{DarF2})$_3$(CN^{n}Bu)$_3$](PF$_6$) (**4a**).* Crude $[Tc(CNp\text{-}FAr^{DarF2})_3(CN^nBu)_2Cl]$ (**3a**) (19 mg, 0.01 mmol) as obtained in the previous preparation was dissolved in tetrahydrofuran (THF) (3 mL), and a solution of $AgPF_6$ (0.06 mmol, 14.4 mg) in MeOH (0.5 mL) was added. The mixture was stirred for 5 min, and the immediately formed colorless precipitate of AgCl was filtered off. CN^{n}Bu (0.5 mmol) was added to the remaining solution. After stirring at room temperature for 30 min, volatiles were removed under reduced pressure. The residue was subsequently washed with water, methanol, and diethyl ether. Single crystals were grown from CH_2Cl_2/*n*-hexane. Pale-green crystals. Yield: 12 mg (0.0056 mmol, 56%). IR (KBr, cm^{-1}): 2967 (w), 2880 (w), 2208 (sh, $\nu_{C\equiv N}$), 2153 (vs, $\nu_{C\equiv N}$), 2110 (m, $\nu_{C\equiv N}$), 2058 (vs, $\nu_{C\equiv N}$), 2033 (vs, $\nu_{C\equiv N}$), 1987 (sh, $\nu_{C\equiv N}$), 1597 (m), 1464(m), 1398 (m), 1364 (s), 1279 (s), 1177 (s), 1138 (s), 904 (m), 847 (s), 708 (m), 683 (m), 637 (w) 557(m). ^{1}H NMR ($CDCl_3$, ppm): 7.91 (8H, s, Aryl-H), 7.79 (2H, Aryl-H), 7.68 (4H, s, Aryl-H), 7.61 (4H, s, Aryl-H) 7.11 (4H, d, ^2J(H−F) = 7.8 Hz, Aryl-H), 2.99−2.85 (6H, m, CH_2−NC), 1.28−1.03 (12H, m, CH_2), 0.81

https://doi.org/10.1021/acs.inorgchem.2c02730
Inorg. Chem. 2022, 61, 16163−16176

Scheme 2. Stepwise Introduction of Distinct Isocyanide Ligands Starting from $(NBu_4)[Tc_2(CO)_6(\mu\text{-}Cl)_3]$

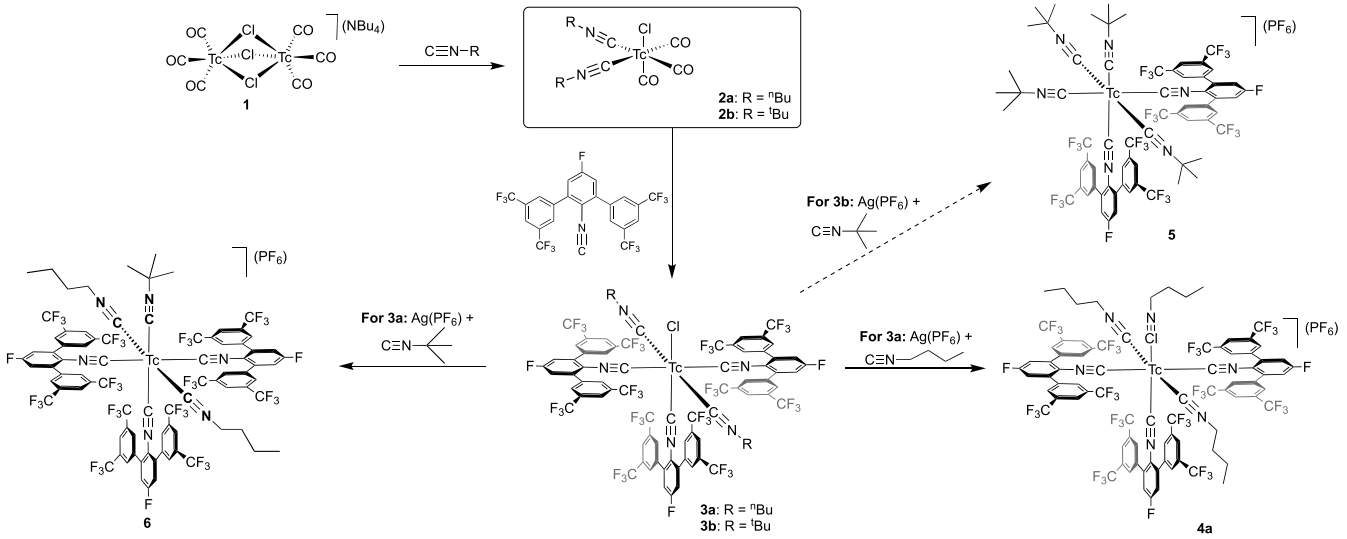

(6H, t, ^3J(H−H) = 7.2 Hz, CH_3), 0.74 (3H, t, ^3J(H−H) = 7.2 Hz, CH_3). ^{19}F NMR ($CDCl_3$, ppm): −62.4 (12F, s, CF_3), −62.6 (24F, s, CF_3), −73.7 (6F, d, ^2J(P−F) = 712 Hz, PF_6), −108.0 (2F, s, *p*-F), −108.3 (1F, s, *p*-F). ^{99}Tc NMR ($CDCl_3$, ppm): −1813 (s, $\nu_{1/2}$ = 410 Hz).

*mer,trans-[Tc(CNp-FAr^{DarF2})$_3$(CN^{n}Bu)$_2$(CN^{t}Bu)](PF$_6$) (**6**).* *mer,trans*-[Tc(CN*p*-FAr^{DarF2})$_3$(CN^{n}Bu)$_2$Cl] (**3a**) (20 mg, 0.01 mmol) was dissolved in THF (3 mL), and a solution of $AgPF_6$ (14.4 mg, 0.06 mmol) in MeOH (0.5 mL) was added. The mixture was stirred at room temperature, and the formed colorless precipitate (AgCl) was filtered off after 30 min. CN^{t}Bu (50 μL, 0.5 mmol) was added to the remaining solution. After 30 min, the liquids were removed under reduced pressure and the remaining solid was washed subsequently with H_2O, Et_2O, and *n*-pentane. Recrystallization from CH_2Cl_2/*n*-hexane gave pale-green crystals. Yield: 15 mg (0.007 mmol, 70%). Single crystals for X-ray diffraction were grown from CH_2Cl_2 layered with *n*-hexane. Alternatively, the synthesis of compound **6** can be performed directly from$(NBu_4)[Tc_2(CO)_6(\mu\text{-}Cl)_3]$ without the isolation of the intermediates **2a** and **3a** with an overall yield of approximately 60%. IR (KBr, cm^{-1}): 2965 (br), 2153 (s, $\nu_{C\equiv N}$), 2104 (m, $\nu_{C\equiv N}$), 2054 (vs, $\nu_{C\equiv N}$), 1597 (w), 1466 (m), 1364 (s), 1279 (s), 1177 (s), 1136 (s), 903 (m), 880 (w), 849 (m) 708 (m), 683 (m), 637 (w), 557 (m). ^{1}H NMR (CD_2Cl_2, ppm): 7.90 (10H, s, aryl-H), 7.80 (4H, s, aryl-H), 7.70 (4H, s, aryl-H), 7.34 (1H, d, ^2J(F−H) = 8 Hz, aryl-H), 7.22 (1H, d, ^2J(F−H) = 8 Hz, aryl-H), 2.96 (4H, t, ^3J(H−H) = 7 Hz, CH_2−NC), 1.18 (8H, m, alkyl-H), 0.87 (9H, s, CH_3), 0.81 (6H, t, ^3J(H−H) = 8 Hz, CH_3). ^{19}F NMR (CD_2Cl_2, ppm): −62.6 (12F, s, CF_3), −62.8 (24F, s, aryl-CF_3), −73.4 (6F, d, ^2J(P−F) = 722 Hz, PF_6), −107.7 (2F, t, ^3J(F−H) = 8 Hz, aryl-pF), −108.2 (1F, t, ^3J(F−H) = 8 Hz, aryl-pF). ^{99}Tc NMR (CD_2Cl_2, ppm): −1821 (s, $\nu_{1/2}$ = 230 Hz).

*[Tc(CNPh^{pF})$_6$](BPh$_4$) (**7**).* CNPh^{pF} (60 μL, 0.50 mmol) was added to a suspension of $(NBu_4)[Tc_2(CO)_6(\mu\text{-}Cl)_3]$ (**1**) (0.05 mmol, 36 mg) in degassed, dry toluene (3 mL). The solution was heated on reflux under argon for 2 h. The resulting solution was filtered, and the volatiles were removed in vacuum. The residue was dissolved in methanol and filtered. A solution of $NaBPh_4$ (170 mg, 0.50 mmol) in MeOH (3 mL) was added to the mixture, which resulted in a colorless precipitate. The solid was filtered off and washed with methanol (3 mL) and diethyl ether (3 mL). Pure **7** was obtained by slow diffusion of *n*-pentane into a THF solution of the complex. The obtained colorless crystals were filtered off, washed with *n*-pentane, and dried under reduced pressure. Yield: 72 mg (0.63 mmol, 63%). IR (KBr, cm^{-1}): 3449 (br), 3055 (w), 2974 (w), 2918 (w) 2851 (w), 2120 (sh), 2085 (s, $\nu_{C\equiv N}$), 1501 (s), 1236 (s) 1153 (w), 833/m) 733 (w), 704 (w), 554 (m), 511(w). ^{1}H NMR (CD_2Cl_2, ppm): 7.41 (12H, m, H−Ar^{pF}), 7.31 (8H, m, H−Ph), 7.13 (12H, t, ^3J(F−H) = 8.4 Hz, H−Ar^{pF}), 7.02 (8H, t, ^3J(H−H) = 7.4 Hz, H−Ph), 6.84 (4H, t, ^3J(H−H) = 7.4 Hz, H−Ph). ^{19}F NMR (CD_2Cl_2, ppm): −109.4 ppm. ^{99}Tc NMR (CD_2Cl_2, ppm): −1888 (s, $\nu_{1/2}$ = 420 Hz).

RESULTS AND DISCUSSION

Reactions of the carbonyltechnetium(I) precursor $(NEt_4)_2[^{99}Tc(CO)_3Cl_3]$ with common alkyl isocyanides such as CN^{t}Bu, CNCy, or CN^{n}Bu in THF or MeOH usually end with the exchange of two Cl^- ligands by isocyanides, and the resulting *fac*-$[^{99}Tc(CO)_3(CNR)_2Cl]$ (**2**) complexes can be isolated in good yields.[34−36] The replacement of the third chlorido ligand is possible, but it requires aqueous conditions or the addition of a chloride scavenger. Using $Ag(PF_6)$, the resulting *fac*-$[Tc(CO)_3(CNR)_3](PF_6)$ salts are obtained in high yields as colorless solids.[36,40] The facial tricarbonyl core remains unaffected by the introduction of the alkyl isocyanides.

The same reactivity was observed for reactions starting from $(NBu_4)[Tc_2(CO)_6(\mu\text{-}Cl)_3]$ (**1**), and products of the composition $[Tc(CO)_3(CNR)_2Cl]$ (**2**) could be isolated as colorless solids (Scheme 2). A completely other reaction pathway was detected for the aromatic, fluorine-substituted isocyanide CN*p*-FAr^{DarF2}, where the decarbonylation product *trans*-[Tc(CO)Cl(CN*p*-FAr^{DarF2})$_4$] is the sole product of the reaction with complex **1**.[46] This remarkable difference stimulated us to study reactions of *fac*-$[Tc(CO)_3(CNR)_2Cl]$ complexes with CN*p*-FAr^{DarF2}.

Indeed, when **2a** or **2b** are exposed to CN*p*-FAr^{DarF2} in boiling toluene, all three carbonyl ligands are replaced and products of the composition *mer,trans*-[Tc(CN*p*-FAr^{DarF2})$_3$(CN^{n}Bu)$_2$Cl] (**3a**) and *mer,trans*-[Tc(CN*p*-FAr^{DarF2})$_3$(CN^{t}Bu)$_2$Cl] (**3b**) are formed (Scheme 2). Their IR spectra clearly confirm the absence of carbonyl ligands and show the vibrations of the isocyanides as three bands in the range between 1925 and 2114 (**3a**) and 1946−2139 (**3b**). The ^{99}Tc NMR resonances of these compounds appear around −1450 ppm and are characterized by extremely large line widths of approximately 20,000 Hz. Such large line widths are unusual for technetium(I) complexes but have been reproducibly found for this type of complexes in different solvents (see the Supporting Information). It is not unusual that the line width of ^{99}Tc NMR spectra increases when the symmetry

https://doi.org/10.1021/acs.inorgchem.2c02730
Inorg. Chem. 2022, 61, 16163−16176

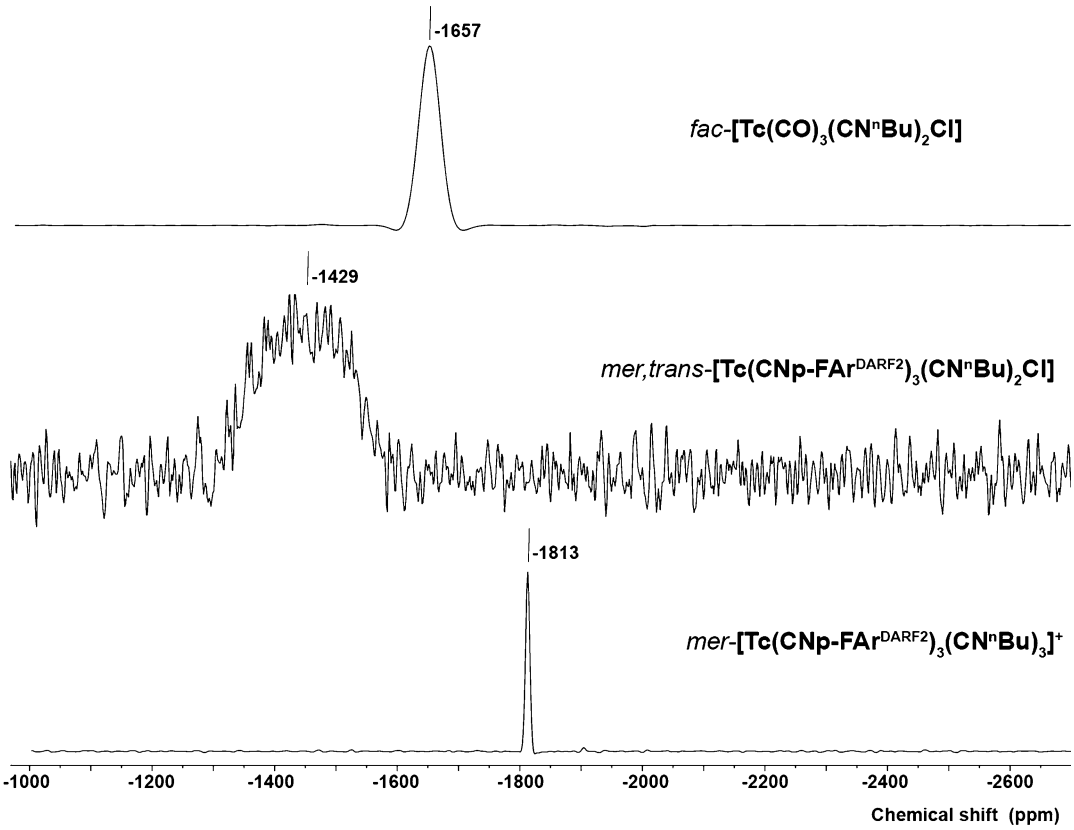

Figure 1. ^{99}Tc NMR spectra of *fac*-[Tc(CO)$_3$(CN^{n}Bu)$_2$Cl] (**2a**) in $CDCl_3$, *mer,trans*-[Tc(CN*p*-FAr^{DarF2})$_3$(CN^{n}Bu)$_2$Cl] (**3a**) toluene, and *mer*-[Tc(CN*p*-FAr^{DarF2})$_3$(CN^{n}Bu)$_3$](PF$_6$) (**4a**) in $CDCl_3$.

around the technetium nucleus decreases, where the narrowest lines with $\nu_{1/2}$ values of only a few Hertz are observed for ideal octahedra such as hexakis(isocyanide)technetium(I) complexes (*vide infra*) or ideal tetrahedra such as pertechnetate.[70] This is also reflected by the spectra shown in Figure 1, where the signal of the trigonal *tris,tris*-complex *mer*-[Tc(CN*p*-FAr^{DarF2})$_3$(CN^{n}Bu)$_3$]$^+$ is narrower than that of the less symmetric compound *mer,trans*-[Tc(CN*p*-FAr^{DarF2})$_3$(CN^{n}Bu)$_2$Cl]. For the extremely large line width of *mer,trans*-[Tc(CN*p*-FAr^{DarF2})$_3$(CN^{n}Bu)$_2$Cl], however, such symmetry considerations seem not to be satisfactory as the sole reason and we assume that also other effects such as ligand rearrangements in solution may play a role.

The replacement of the facially arranged carbonyls in **2** by the bulky CN*p*-FAr^{DarF2} ligands results in a rearrangement of the entire coordination sphere in a way that the incoming CN*p*-FAr^{DarF2} ligands adopt meridional positions and the remaining CN^{n}Bu or CN^{t}Bu ligands are found in the products in trans-position to each other. This gives a markedly distorted octahedral coordination sphere for the technetium atom with deviations of the respective cis-angles from the ideal octahedral angles by up to 9°. Figure 2 illustrates the molecular structure of compound **3b**. Selected bond lengths and angles are summarized in Table 1.

While the remaining chlorido ligand in the carbonyl complex **2b** can readily be replaced by a third CN^{t}Bu ligand,[40] this is not the case for complex **3a**. The addition of Ag(PF$_6$) to a solution of **3a** in a THF/MeOH mixture results in the precipitation of the AgCl, which could be removed by filtration. After the addition of CN^{t}Bu to the filtrate, the formation of at least two new Tc(I) species could be detected by ^{99}Tc NMR spectroscopy, but all our attempts to isolate the target complex *mer*-[Tc(CN*p*-FAr^{DarF2})$_3$(CN^{t}Bu)$_3$](PF$_6$) failed up to now. After prolonged heating of the reaction mixture, however, a small amount of pale-green single crystals were isolated. They could be identified as *cis*-[Tc(CN*p*-FAr^{DarF2})$_2$(CN^{t}Bu)$_4$](PF$_6$) (**5**) by X-ray diffraction. The molecular structure of this compound and some selected bond lengths and angles are given as Supporting Information. Since only a tiny amount of this product was available, no spectroscopic data could be collected. Thus, this product shall not be discussed here in detail. We regard its formation under the described conditions and the fact that we were not able to isolate a product with three CN*p*-FAr^{DarF2} and CN^{t}Bu ligands, respectively, as a strong indicator for a steric overload of the coordination sphere by these bulky ligands.

The assumption that mainly steric factors are responsible for the unavailability of *mer*-[Tc(CN*p*-FAr^{DarF2})$_3$(CN^{t}Bu)$_3$](PF$_6$) is supported by the fact that a corresponding *tris*, *tris*-complex with the less bulky CN^{n}Bu ligand could be isolated following the procedure described above in satisfactory yields. Single crystals of *mer*-[Tc(CN*p*-FAr^{DarF2})$_3$(CN^{n}Bu)$_3$](PF$_6$) (**4a**) were obtained from CH_2Cl_2/n-hexane. Figure 3 depicts the structure of the cation of **4a**, and selected bond lengths and angles are listed in Table 1. The space-filling models in Figure 3b,c clearly show that the structural flexibility of the *n*-butyl residues is required to place three of such isocyanides in the gaps left by the CF_3 groups of the meridionally arranged CN*p*-FAr^{DarF2} ligands. Bond lengths and angles in the coordination sphere of technetium are not significantly influenced by the steric hindrance induced by the CN*p*-FAr^{DarF2} ligands. This comes not completely surprising since due to the meta-

https://doi.org/10.1021/acs.inorgchem.2c02730
Inorg. Chem. 2022, 61, 16163−16176

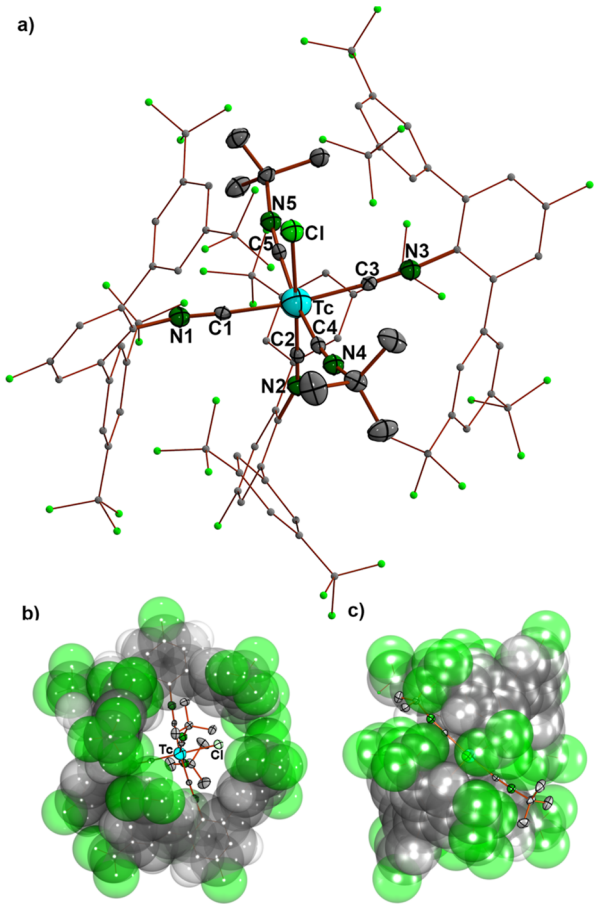

Figure 2. (a) Molecular structure of *mer,trans*-[Tc(CN*p*-FAr^{DarF2})$_3$(CN^{t}Bu)$_2$Cl] (**3b**) and space-filling representation of the molecule (b) along the CN^{t}Bu-Tc-CN^{t}Bu axis and (c) along the Cl−Tc axis (spheres represent carbon and fluorine atoms with their vdW radii).

positions of the CF_3 substituents in their respective phenyl rings, the fluorine atoms are more than 4 Å apart from technetium. They, thus, form a kind of "outer-sphere" protective shell, which is nicely illustrated in Figures 2b and 3b.

The fact that we could not isolate a cation of the composition *mer*-[Tc(CN*p*-FAr^{DarF2})$_3$(CN^{t}Bu)$_3$](PF$_6$) and the structural flexibility of CN^{n}Bu demonstrated in the formation of **4a** raised the question about the replacement of the chlorido ligands in compounds of type **3** by a third isocyanide ligand with a different steric bulk. Following the protocol applied for the synthesis of **4a**, we could remove the Cl^- ligand of complex **3a** by the addition of Ag(PF$_6$) in THF and fill the vacant coordination site with CN^{t}Bu. Pale-green crystals could be isolated and characterized as *mer,trans*-[Tc(CN*p*-FAr^{DarF2})$_3$(CN^{n}Bu)$_2$(CN^{t}Bu)](PF$_6$) (**6**). The $\nu_{C\equiv N}$ absorptions appear at 2054, 2104, and 2163 cm^{-1}, and the ^{99}Tc NMR spectrum of the compound is characterized by a relatively narrow line ($\nu_{1/2}$ = 230 Hz) at −1821 ppm in CD_2Cl_2. This is in the same spectral range as observed for other Tc(I) complexes with six isocyanide ligands in their coordination sphere.[3,4,11,70] The small line width reflects the high symmetry of the first coordination sphere of the ^{99}Tc nucleus.[70] Figure 4 depicts the structure of the cation of complex **6**. Selected bond lengths and angles for the compound are contained in Table 1 and compared with the values of complexes **3a** and **4a**.

Table 1. Selected Bond Lengths (Å) and Angles (degrees) in *mer,trans*-[Tc(CN*p*-FAr^{DarF2})$_3$(CN^{t}Bu)$_2$Cl] (3b), *mer*-[Tc(CN*p*-FAr^{DarF2})$_3$(CN^{n}Bu)$_3$](PF$_6$) (4a), and *mer,trans*-[Tc(CN*p*-FAr^{DarF2})$_3$(CN^{t}Bu)](CN^{n}Bu)$_2$](PF$_6$) (6)

	(3b)	(4a)	(6)
Tc-C1	2.008(3)	2.02(1)	2.03(2)
Tc-C2	1.897(3)	1.969(8)	1.983(5)
Tc-C3	2.023(3)	2.03(1)	2.02(1)
Tc-C4	2.064(3)	2.07(1)	2.039(9)
Tc-C5	2.027(3)	2.05(1)	2.060(7)
Tc-C6/Cl	2.5067(7)	2.06(1)	2.039(9)
C1-Tc-C2	91.7(1)	88.9(4)	90(4)
C1-Tc-C3	182.9(1)	177.5(4)	175(4)
C1-Tc-C4	93.8(1)	86.9(4)	88(2)
C1-Tc-C5	89.7(1)	92.4(4)	92(2)
C1-Tc-C6/Cl	87.21(7)	93.1(4)	88(4)
C2-Tc-C3	94.7(1)	93.5(4)	93(3)
C2-Tc-C4	97.3(1)	95.6(4)	91.5(3)
C2-Tc-C5	90.6(1)	89.8(4)	94.3(3)
C2-Tc-C6/Cl	176.91(8)	175.1(4)	173.2(3)
C3-Tc-C4	88.4(1)	93.7(4)	96(2)
C3-Tc-C5	90.6(1)	86.8(4)	83(2)
C3-Tc-C6/Cl	86.19(7)	84.5(4)	89(3)
C4-Tc-C5	171.3(1)	174.6(5)	174.2(3)
C4-Tc-C6/Cl	85.55(8)	89.1(4)	81.9(3)
C5-Tc-C6/Cl	86.53(8)	85.6(4)	92.3(3)

mer,trans-[Tc(CN*p*-FAr^{DarF2})$_3$(CN^{n}Bu)$_2$(CN^{t}Bu)](PF$_6$) (**6**) is to the best of our knowledge the first structurally characterized complex with three different isocyanide ligands in well-defined positions in the coordination sphere of a transition metal. Previous attempts to synthesize such compounds ended with the formation of a mixture of hexakis(isocyanide)technetium(I) species with a statistical distribution of the ligands added during the complex formation.[11] This has also been found for reactions between the Tc(III) complex [Tc(tu)$_6$]Cl$_3$ and a mixture of CN^{n}Bu and CN^{t}Bu, which give mixtures of [Tc(CN^{n}Bu)$_{6-n}$(CN^{t}Bu)$_n$]$^+$ cations. They can readily be detected by their ^{99}Tc NMR signals (Figure 5). The fractions of the individual complexes can be controlled by the percentage of the two isocyanides used. When the mixed-ligand hexakis(isocyanide) complexes are once formed, they do not undergo further ligand exchange with the competing ligand, as has been proven by an attempted reaction of [Tc(CN^{n}Bu)$_6$]$^+$ with an excess of CN^{t}Bu.

Finally, the question of why the carbonyl ligands of compounds **2** are readily and completely replaced during reactions with CN*p*-FAr^{DarF2} and a *mer*-{Tc^I(CN*p*-FAr^{DarF2})$_3$}$^+$ core is formed, while no such reactions were observed for CN^{n}Bu, CN^{t}Bu, or CNCy remains. The fact that isocyanides should not be regarded as simple "CNR surrogates" of carbonyl ligands has been well accepted for a long time, and several examples of carbonyl/isocyanide exchange reactions have been reported.[42,71−76] In the chemistry of the group 7 elements, however, such replacements are mainly restricted to labilized carbonyl ligands.[29−32,43,77−83] The coordination properties of isocyanides are obviously governed by a complex interplay of their molecular orbitals. This results in substitution-specific and difficult-to-predict σ-donor and π-acceptor properties for the individual ligands, which may interfere additionally with restrictions given by the steric bulk of the residues.[48] In a rough approximation, the presence of

https://doi.org/10.1021/acs.inorgchem.2c02730
Inorg. Chem. 2022, 61, 16163−16176

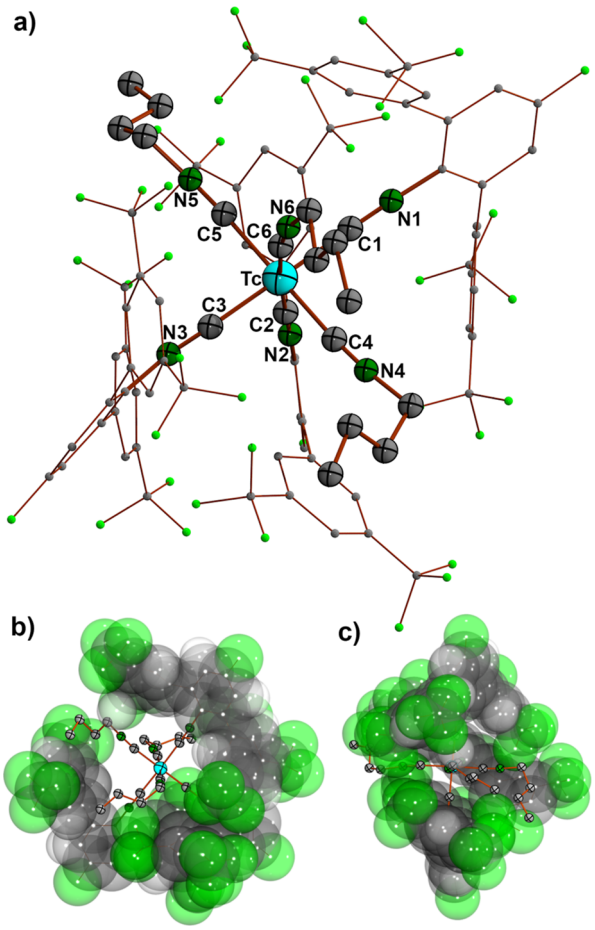

Figure 3. (a) Structure of the *mer*-$[Tc(CNp\text{-}FAr^{DarF2})_3(CN^nBu)_3]^+$ cation of **4a** and space-filling representation of the cation (b) along the CN^nBu-Tc-CN^nBu axis and (c) along the CN^nBu-Tc-CN*p*-FAr^{DarF2} axis (spheres represent carbon and fluorine atoms with their vdW radii).

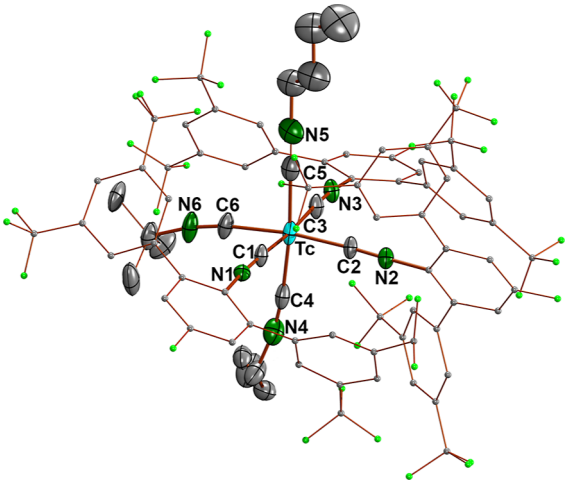

Figure 4. (a) Structure of the cation of *mer,trans*-$[Tc(CNp\text{-}FAr^{DarF2})_3(CN^nBu)_2(CN^tBu)](PF_6)$ (**6**).

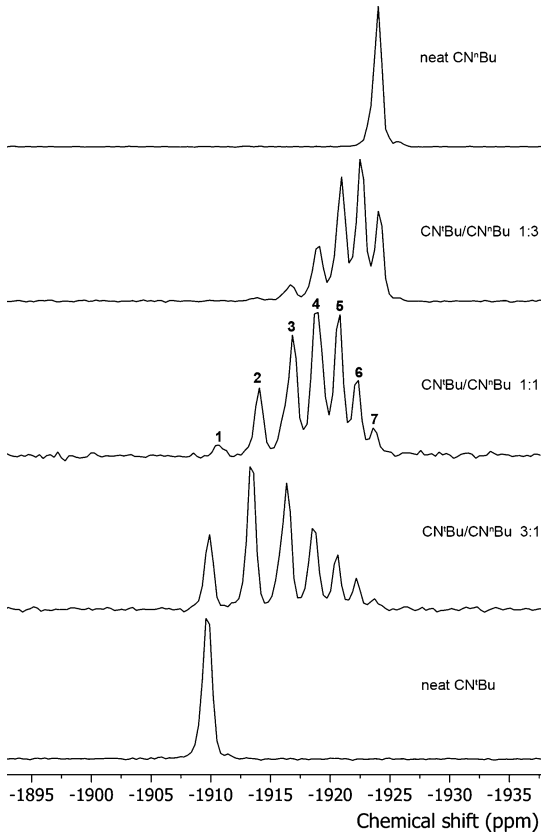

Figure 5. ^{99}Tc NMR spectra of mixed-ligand $[Tc(CN^nBu)_{6-n}(CN^tBu)_n]^+$ complexes formed from reactions of $[Tc(tu)_6]Cl_3$ with different ratios of CN^nBu and CN^tBu. A tentative assignment of the observed signals to individual species is given for the 1:1 reaction: **1** $[Tc(CN^tBu)_6]^+$, **2** $[Tc(CN^nBu)(CN^tBu)_5]^+$, **3** $[Tc(CN^nBu)_2(CN^tBu)_4]^+$, **4** $[Tc(CN^nBu)_3(CN^tBu)_3]^+$, **5** $[Tc(CN^nBu)_4(CN^tBu)_2]^+$, **6** $[Tc(CN^nBu)_5(CN^tBu)]^+$, and **7** $[Tc(CN^tBu)_6]^+$.

electron-withdrawing substituents may correlate with stronger acceptor properties and weaker donor properties, but there exists an increasing number of examples, where details of the ligation of isocyanides cannot be described on the basis of spectroscopic data such as IR frequencies or bond lengths (and angle) considerations. Co-ligands present in the coordination sphere of the considered complexes, but also the charge distribution and accessibility on the surface of the donor atom, seem to play a crucial role in the estimation of the electronic situation of coordinated isocyanides and (more importantly) the reactivity of the individual proligands.

A correlation between some properties of isocyanides and their highest occupied molecular orbital (HOMO) and lowest unoccupied molecular orbital (LUMO) has been argued in some specific cases in the past.[84−87] The LUMO in a sense corresponds to regions of partial positive polarization, and the HOMO corresponds to electron-rich regions of the molecule. Electrostatic potential energy calculations are generally accepted as valuable qualitative and quantitative predictive tools giving insights into the nucleophilicity (electron-richness) and electrophilicity (electron-deficiency) of certain atoms or fragments in molecules.[88−90] As such, it is surprising that they have not yet been applied to the σ-donation/π-back-donation problem and we envisioned a good descriptor for the combined donor−acceptor behavior of potential isocyanide ligands derived from computed electrostatic potential energy data. We therefore modeled several (potential) isocyanide ligands by DFT calculations at the B3LYP/6-311++G** level. The full convergence of the structure optimizations was verified by the absence of negative frequencies in the following

https://doi.org/10.1021/acs.inorgchem.2c02730
Inorg. Chem. 2022, 61, 16163−16176

frequency calculations. NBO calculations revealed that the electron configuration of the potential carbon donor atoms was interestingly not a reasonable descriptor of the experimentally observed reactivity. The final self-consistent field (SCF) densities were converted into cube data for electron densities and electrostatic potentials of equivalent cube sizes for all compounds. From these, mappings of the electrostatic potentials onto the density isosurfaces (MO = 0.02; ρ = 0.004) were generated and they revealed stunning substitution-dependent differences when normalized to the potential boundaries [e/Å^3] of the intermediate donor CNMe. The electrostatic potential in this case corresponds to the potential energy difference obtained for moving a positive point charge along a grid on the van der Waals (vdW) surface of the molecule (more precisely, on the density level that is indicated). Thus, positive values of electrostatic potential correspond to the repulsion of the positive charge. These regions are therefore themselves considered to be positively polarized. Negative values in potential energy correspond to the attraction of the positive charge, and hence, these regions are themselves considered to be negatively polarized. The corresponding electrostatic potential maps for the isocyanides discussed in this paper are shown in Figure 6, while the Supporting Information contains the maps for some other isocyanides.

For isocyanides, it is reasonable to assume that electron-deficient regions on the surface of the isocyano carbon atom would enable improved π-back-donation, while electron-rich regions on the surface of the same carbon atom are responsible for a better σ-donation. At the same time, the steric restraints on the donor carbon atom can be partially included in such an approach by averaging the obtained potential energies over the accessible surface of the potential donor atoms. Accessible surface in this case means the surface on the vdW boundary of a specific atom but not in the vdW boundary of another atom. The positive sites on carbon are more diffuse and approximately located at the antibonding π^*_{CN} orbital lobes, while the negative charge is situated at the carbon atoms lone-pair (n_C orbital) and much more directional/focused and aligned with the CN bond axis. Based on these visual results, we calculated the electrostatic and steric surface properties of the carbon atoms involved in isocyanide−metal binding.[90] The sterically demanding isocyanides expectedly show less overall accessible surface area, while the less encumbered isocyanides have a larger overall accessible carbon surface. In a similar way, the rather electron-accepting isocyanides (partial π-acceptors) show an increased positive surface area at the potential donor carbon atom compared to the rather σ-donor ligands that have no positive surface exposure on their isocyanide carbon atom. The charge distribution on the surface also plays a crucial role in the interplay between π-acceptance and σ-donation. As a simple descriptor for the overall donor/acceptor properties of the isocyanides, we determined the quotient from a sum parameter containing the calculated potential energy extrema and the averaged potential energy on the vdW surface of the carbon donor atoms (kcal/mol) and the exposed vdW surface area (Å^2): the surface-averaged donor−acceptor potential (SADAP) (eq 1). The results for the isocyanides discussed in the present study are summarized in Table 2, while an extended version of the table with many more isocyanides is contained in the Supporting Information.

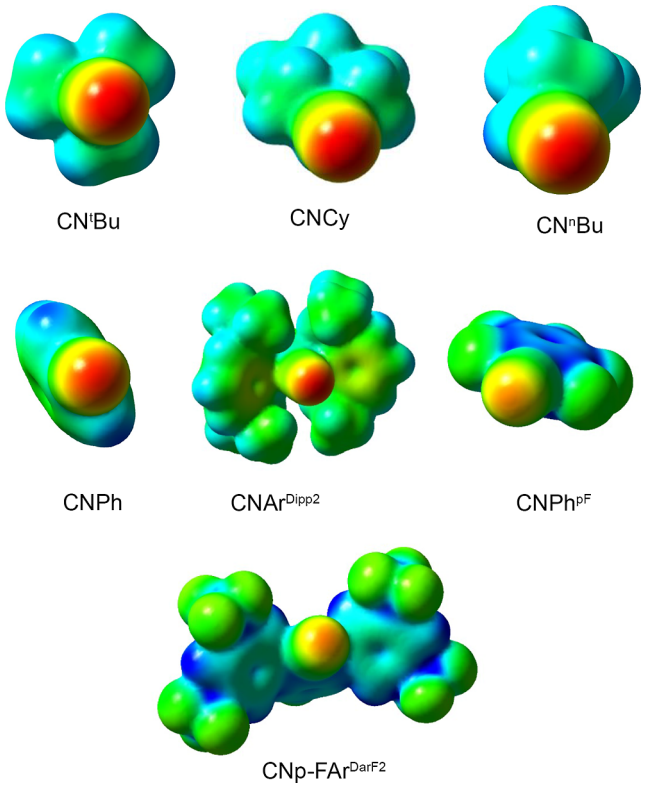

Figure 6. Electrostatic potential mapping (MO = 0.02; ρ_{iso} = 0.004) normalized to the potential boundaries of CNMe ($\pm 7.478 \times 10^{-2}$ [e/Å^3]; blue = positive, red = negative) for the isocyanides discussed in this paper.

$$\mathrm{SADAP} = \frac{\mathrm{EP_{min}} + \mathrm{EP_{max}} + \mathrm{AP}}{\mathrm{ES_{pos}} + \mathrm{ES_{neg}}} \quad (1)$$

The derived sum parameter corresponds to the average interaction energy of the isocyanide carbon atom with positively and negatively charged moieties over its entire accessible surface. Much to our delight, the obtained SADAP values correlate well with the observed reactivity of the ligands. Ligands with a progressively positive overall sum parameter can easily and rapidly replace CO ligands on low-valent metal complexes while those having negative sum parameters are σ-donors with predominantly neglectable back-bonding properties. Consequently, no or only a slow exchange of carbonyl ligands is observed with the latter group of isocyanides. In practice, uncoordinated isocyanides with pronounced π-accepting behavior are frequently more chemically reactive relative to their more σ-donating relatives. A good example in this regard is the reported decomposition of pentafluorophenyl isocyanide (CNC_6F_5) at temperatures above 13 °C,[91] whereas phenyl isocyanide (CNPh) is a stable entity at room temperature both as a pure substance or in solution. Accordingly, compounds with intermediate sum parameters are especially interesting since they should be more thermally stable as compared to their highly π-accepting analogs while still exhibiting pronounced π-acceptance. These compounds with intermediate parameters bind tightly to low-valent metal ions due to their considerable π-acceptance combined with strong σ-donation without the sensitivity observed for the highly π-deficient isocyanides. It has not escaped our notice that SADAP values could easily be adopted for the evaluation

https://doi.org/10.1021/acs.inorgchem.2c02730
Inorg. Chem. 2022, 61, 16163−16176

Table 2. Calculated Electrostatic Potential Surface Properties of the Isocyanide Carbon Atom at the vdW Boundary for Structures Optimized at the B3LYP/6-311++G Level[a]**

	exposed vdW surface, ES (Å^2)		extrema for potential energies at vdW surface, EP (kcal/mol)		average potential energies at vdW surface, AP (kcal/mol)	surface-averaged donor atom potential SADAP, (kcal/mol Å^2)
isocyanide	ES_{pos}	ES_{neg}	EP_{min}	EP_{max}	$AP_{overall}$	SADAP
$CNAr^{Dipp2}$	0.00	22.13	−37.64	−8.87	−26.04	−3.28
CN^tBu	0.00	31.43	−39.63	−5.86	−22.00	−2.15
CNCy	0.00	31.61	−39.23	−5.09	−21.81	−2.09
CN^nBu	0.00	31.58	−38.51	−5.52	−21.36	−2.07
CNH	0.00	31.12	−31.48	−4.62	−16.42	−1.69
CNPh	0.05	31.28	−35.20	1.72	−18.01	−1.64
$CNPh^{pF}$	1.67	29.53	−32.02	7.05	−14.10	−1.25
CN*p*-FAr^{DarF2}	20.50	6.74	−11.49	69.07	16.88	2.73

[a]Surface properties were evaluated at the ρ = 0.001 level using an electrostatic potential map basis with a grid-point spacing of 0.25. The last column contains the SADAP = $(EP_{min} + EP_{max} + AP)/(ES_{pos} + ES_{neg})$ as a combined descriptor of steric and electrostatic properties of the potential ligands, which allows an estimation of their reactivity.

and reactivity prediction of ligand classes other than isocyanides.

The same maps were also generated for the potential boundaries [e/Å^3] of CO. However, since nearly all isocyanides show higher electron density at the donor carbon atom compared to CO (and thus can be considered much stronger σ-donors), the differences are less pronounced but still obvious. The visual identification of the bonding properties of CO in comparison to the isocyanides may be illustrative (see the Supporting Information) but should not be overevaluated. The same holds true for the numerical SADAP value of 0.11 kcal/Å^2, which necessarily comes close to zero due to the balanced charge distribution on the surface of its almost freely available carbon atom.

Although the SADAP parameters introduced in Table 2 may represent only a rough approximation to the real electronic and steric situations at the isocyanide carbon atoms, they reflect the observed reactivity of the ligands surprisingly well. Thus, isocyanides with pronounced negative SADAP values such as alkyl isocyanides or the highly sterically encumbered alkyl-substituted *m*-terphenyl isocyanides (see $CNAr^{Dipp2}$ in Table 2 and more examples in the Supporting Information) do not replace carbonyl ligands from the *fac*-$\{Tc(CO)_3\}^+$ core but form mixed CO/CNR complexes.[30−35] When the steric requirements of the incoming isocyanide ligands make cis coordination unfavorable, they are directed in trans-positions, and the *mer*-$\{Tc(CO)_3\}^+$ core is formed, as has been observed for $CNAr^{Dipp2}$ (see also Scheme 1).[41,45] On the other hand, the isocyanide of our series with the most positive SADAP value, CN*p*-FAr^{DarF2}, readily reacts with *fac*-$\{Tc(CO)_3\}^+$ starting materials such as $(NBu_4)[Tc_2(CO)_6(\mu\text{-}Cl)_3]$ or $(NEt_4)_2[Tc(CO)_3Cl_3]$ to form *trans*-$[Tc(CO)Cl(CN\text{-}p\text{-}FAr^{DarF2})_4]$ with four of the bulky isocyanides in the equatorial plane.[46] This behavior is in line with the findings of the present study, where CN*p*-FAr^{DarF2} replaces the three carbonyl ligands of compounds **2** and reorganizes the coordination sphere of technetium. Steric restriction due to the two butyl isocyanide ligands of **2** prevents the introduction of a fourth CN*p*-FAr^{DarF2} ligand in this case. This indicates that the reactivity of CN*p*-FAr^{DarF2} should be mainly determined by the fluorine substitution on the central phenyl ring and suggests that *p*-fluorophenyl isocyanide, $CNPh^{pF}$, may show a similar reactivity.

Indeed, during reactions of **1** or **2b** with $CNPh^{pF}$, a complete replacement of the coordination sphere of technetium and the formation of the $[Tc(CNPh^{pF})_6]^+$ cation is observed (Scheme 3). The reactions proceed stepwise, as has been confirmed by a

Scheme 3. Synthesis of $[Tc(CNPh^{pF})_6](BPh_4)$

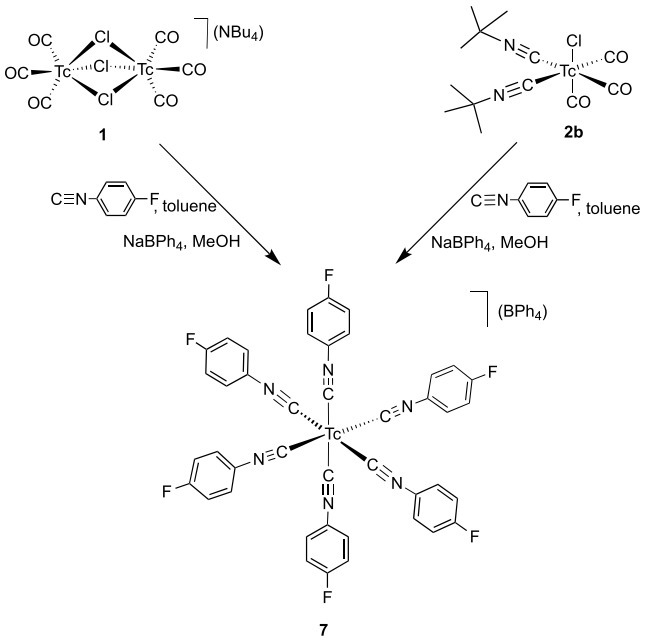

subsequent recording of ^{99}Tc and ^{19}F NMR spectra. The spectra of such a reaction sequence are given in the Supporting Information together with a tentative assignment of the signals to individual mixed-ligand species. The final product, $[Tc(CNPh^{pF})_6]^+$, could be isolated as its BPh_4^- salt in the form of colorless crystals. Single crystals for X-ray diffraction were obtained from THF/n-pentane.

Despite the fact that ^{99m}Tc-Sestamibi, $[Tc(MIBI)_6]^+$, is one of the most-used diagnostic radiopharmaceuticals worldwide and many other hexakis(isocyanide)technetium(I) complexes have been prepared and studied chemically and spectroscopically,[3−8] there is only one entry of such a compound in the CSD database,[92] and the structure of another compound is briefly described in a conference report.[93] Thus, we

https://doi.org/10.1021/acs.inorgchem.2c02730
Inorg. Chem. 2022, 61, 16163−16176

determined the structure of complex **7** by X-ray diffraction. Figure 7 contains an ellipsoid depiction of the complex cation.

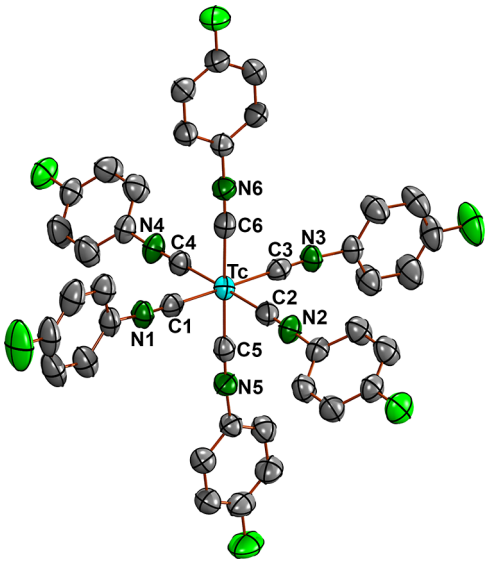

Figure 7. Structure of the complex cation of $[Tc(CNPh^{pF})_6](BPh_4)$ (**7**). Hydrogen atoms have been omitted for clarity. Thermal ellipsoids represent 50% probability.

Expectedly, the coordination sphere of technetium is almost ideally octahedral with maximum deviations of 2.8° for the cis-angles and 3.4° for the trans-angles (for details, see the Supporting Information). The Tc−C−N angles are also almost linear (maximum deviation: 3.6°).

The IR spectrum of $[Tc(CNPh^{pF})_6](BPh_4)$ shows a $\nu_{C\equiv N}$ band at 2085 cm^{-1}, and a narrow ($\nu_{1/2}$ = 420 Hz) ^{99}Tc NMR signal in CH_2Cl_2 appears at −1857 ppm. This value is close to that of the $[Tc(CNPh)_6]^+$ cation in $CDCl_3$ (−1889 ppm). This means that the ^{99}Tc nucleus seems to be appreciably deshielded relative to those of hexakis technetium(I) complexes with alkyl isocyanides, which show ^{99}Tc NMR signals between −1914 and −1964 ppm.[94]

While differences between alkyl and (sterically unencumbered) aryl isocyanides are suggested by the SADAP parameters of Table 2, the values indicate that some isocyanides may display similar reactivity patterns. For example, the SADAP values suggest that the reactivity observed for $CNPh^{pF}$ might also be replicated for the unsubstituted phenyl isocyanide, CNPh. Such an expectation is supported by recent reports, which describe the exchange of one carbonyl ligand of $[^{99m}Tc(CO)_3(OH_2)_3]^+$ during reactions with substituted phenyl isocyanides and the formation of $[^{99m}Tc(CO)_2(CNPh^R)_4]^+$ complexes.[95−97] It should, however, be noted that, due to the different concentration levels of reaction with ^{99}Tc and ^{99m}Tc (millimolar vs nanomolar) and the related huge ligand excess in the latter ones, the course of such reactions is not always identical. During attempted reactions between $(NBu_4)[Tc_2(CO)_6(\mu\text{-}Cl)_3]$ and phenyl isocyanide (CNPh), we could indeed observe the formation of small amounts of $[Tc(CNPh)_6]^+$ by ^{99}Tc NMR spectroscopy. We were, however, not able to isolate considerable amounts of the product since an ongoing decomposition of the sensitive isocyanide was observed. Given that $CNPh^{pF}$ readily replaces the CO ligands in $(NBu_4)[Tc_2(CO)_6(\mu\text{-}Cl)_3]$, while the identical ligand substitution with CNPh does not proceed with the same efficiency, it is reasonable to suggest that a SADAP value of ca. −1.50 kcal/mol Å^2 may represent a threshold boundary for the substitution of carbonyl ligands by isocyanides. However, additional ligand substitution experiments are required to further refine this notion.

CONCLUSIONS

Defined mixed-isocyanide complexes of technetium(I) can be prepared by a stepwise ligand-exchange procedure starting from *fac*-$[Tc(CO)_3(CNR)_2Cl]$ complexes. Steric and electronic parameters give control over the possible ligand exchange rate. Thus, only the three carbonyl ligands of *fac*-$[Tc(CO)_3(CNR)_2Cl]$ complexes are replaced by the *p*-fluorinated CN*p*-FAr^{DarF2} ligands due to steric restrictions. This takes place under a rearrangement of the coordination sphere of technetium in a way that the incoming ligands are directed into meridional positions. The already present alkyl isocyanides remain in the coordination sphere of the metal. A completely different course of the reaction is observed when the steric limitations of the CN*p*-FAr^{DarF2} are "removed" without changing significantly the electronic properties of the ligand, which are dominated by the fluorine atom in the trans-position to the isocyanide. This means that similar reactions with $CNPh^{pF}$ end with a complete occupation of the coordination sphere of technetium with *p*-fluorophenyl isocyanide and the formation of the $[Tc(CNPh^{pF})_6]^+$ cation.

Table 3. IR Frequencies of the ν_{CN} Stretches in the Complexes under Study

	CN^nBu	CN*p*-FAr^{DarF2}	CN^tBu	$CNPh^{pF}$	$CNAr^{Dipp2}$
uncoordinated isocyanide	**2149**	**2119**	**2135**	**2129**	**2124**
2a[a]	2208, 2372				
2b[b]			2208, 2190		
$[Tc(CO)_3(CN^tBu)_3](NO_3)$[c]			2215, 2185		
3a		1946, 2048, 2139			
3b			1925, 2031, 2114		
4a		2033, 2058, 2153			
6			2054, 2104, 2153		
7				2085	
$[Tc(CN^tBu)_6](PF_6)$[d]			2080		
$[Tc(CO)(CN\text{-}p\text{-}FAr^{DarF2})_4Cl]$[e]		1982, 2064			
$[Tc(CO)_3(CNAr^{Dipp2})_2Cl]$[f]					2152

[a]CO bands at 1935, 1985, and 2046 cm^{-1}. [b]CO bands at 1909, 1977, and 2049 cm^{-1}, ref 34. [c]CO bands at 2003 and 2062 cm^{-1}, ref 40. [d]Reference 4. [e]CO bands at 1935 cm^{-1}, ref 46. [f]CO bands at 1938, 1989, and 2039 cm^{-1}, ref 41.

https://doi.org/10.1021/acs.inorgchem.2c02730
Inorg. Chem. 2022, 61, 16163−16176

Interesting changes in the σ-donor/π-acceptor properties of the isocyanides in the course of such ligand exchange reactions are observed. While (on the basis of the ν_{CN} frequencies of the isocyanides) in mixed carbonyl/isocyanide complexes, back-donation preferably takes place into the π-orbitals of the carbonyl ligands, the corresponding ν_{CN} frequencies shift to higher energies with respect to their positions in the IR spectra of the uncoordinated isocyanides.

The situation necessarily changes when the carbonyls are replaced by CN*p*-FAr^{DarF2} ligands and the ν_{CN} stretches of the hexakis and mixed-isocyanide complexes indicate a larger degree of π-acceptor behavior of isocyanides, which can be deduced from the observed bathochromic shifts. The experimental ν_{CN} frequencies are summarized in Table 3, which also contains some previously measured data for comparison. A clear situation is observed for the homoleptic complexes $[Tc(CN^tBu)_6]^+$ and $[Tc(CNPh^{pF})_6]^+$, where bathochromic shifts of approximately 50 cm^{-1} clearly support back-donation. Interestingly, some π-acceptor behavior also seems to be present in *trans*-$[Tc(CO)Cl(CNp\text{-}FAr^{DarF2})_4]$,[46] where the presence of only one carbonyl ligand seems to be insufficient to compensate for the charge density from the d^6 ion alone. It would be interesting to evaluate the individual contributions of the different isocyanides in the mixed-isocyanide complexes **3**, **4**, **5**, and **6**, but unfortunately, a reliable assignment of the bands is not possible on the basis of the present data. Perhaps, future isotope labeling experiments or ^{13}C NMR experiments with related rhenium compounds may clarify these questions.

■ ASSOCIATED CONTENT

Supporting Information

The Supporting Information is available free of charge at https://pubs.acs.org/doi/10.1021/acs.inorgchem.2c02730.

Crystallographic tables, bond lengths and angles, ellipsoid plots, spectroscopic data, and DFT results (PDF)

Accession Codes

CCDC 2176651−2176654 and 2176657 contain the supplementary crystallographic data for this paper. These data can be obtained free of charge via www.ccdc.cam.ac.uk/data_request/cif, or by emailing data_request@ccdc.cam.ac.uk, or by contacting The Cambridge Crystallographic Data Centre, 12 Union Road, Cambridge CB2 1EZ, UK; fax: +44 1223 336033.

■ AUTHOR INFORMATION

Corresponding Authors

Joshua S. Figueroa − *Department of Chemistry and Biochemistry, University of California, San Diego, San Diego, California 92093, United States;* orcid.org/0000-0003-2099-5984; Email: jsfig@ucsd.edu

Ulrich Abram − *Freie Universität Berlin, Institute of Chemistry and Biochemistry, Berlin 14195, Germany;* orcid.org/0000-0002-1747-7927; Email: ulrich.abram@fu-berlin.de

Authors

Guilhem Claude − *Freie Universität Berlin, Institute of Chemistry and Biochemistry, Berlin 14195, Germany*

Jonas Genz − *Freie Universität Berlin, Institute of Chemistry and Biochemistry, Berlin 14195, Germany*

Dominik Weh − *Freie Universität Berlin, Institute of Chemistry and Biochemistry, Berlin 14195, Germany*

Maximilian Roca Jungfer − *Freie Universität Berlin, Institute of Chemistry and Biochemistry, Berlin 14195, Germany*

Adelheid Hagenbach − *Freie Universität Berlin, Institute of Chemistry and Biochemistry, Berlin 14195, Germany*

Milan Gembicky − *Department of Chemistry and Biochemistry, University of California, San Diego, San Diego, California 92093, United States*

Complete contact information is available at: https://pubs.acs.org/10.1021/acs.inorgchem.2c02730

Notes

The authors declare no competing financial interest.

■ ACKNOWLEDGMENTS

We gratefully acknowledge financial support from the DFG (Deutsche Forschungsgemeinschaft: Graduated School BIOQIC), the U.S. National Science Foundation (International Supplement to CHE-1802646), and the Alexander von Humboldt Foundation (Fellowship to J.S.F.). We acknowledge the assistance of the Core Facility BioSupraMol supported by the DFG and thank the High-Performance Computing Centre of the Zentraleinrichtung für Datenverarbeitung of the Freie Universität Berlin for computational time.

■ REFERENCES

(1) Kronauge, J. F. K.; Mindiola, D. J. The value of Stable Metal-Carbon Bonds in Nuclear Medicine and the Cardiolite Story. *Organometallics* **2016**, *35*, 3432−3435.

(2) IAEA Technical Reports Series No. 466. *Technetium-99m Radiopharmaceuticals: Manufacture of Kits*; International Atomic Energy Agency: Vienna, 2008, pp 126−129.

(3) Abrams, M. J.; Davison, A.; Jones, A. G.; Costello, C. H.; Pang, H. Synthesis and Characterization of Hexakis(alkyl isocyanide) and Hexakis(aryl isocyanide) Complexes of Technetium(I). *Inorg. Chem.* **1983**, *22*, 2798−2800.

(4) Abrams, M. J.; Davison, A. R.; Faggiani, A. G.; Jones, C. J. L.; Lock, C. J. L. Chemistry and Structure of Hexakis(thiourea-S)technetium(III) Trichloride Tetrahydrate, $[Tc(SC(NH_2)_2)_6]Cl_3 \cdot 4H_2O$. *Inorg. Chem.* **1984**, *23*, 3284−3288.

(5) Herman, L. W.; Sharma, V.; Kronauge, J. F.; Barbarics, E.; Herman, L.; Piwnica-Worms, D. Novel Hexakis(areneisonitrile)-technetium(I) Complexes as Radioligands Targeted to the Multidrug Restistance P-Glycoprotein. *J. Med. Chem.* **1995**, *38*, 2955−2963.

(6) Piwnica-Worms, D.; Kronauge, J. F.; Holman, B. L.; Davison, A.; Jones, A. G. Comparative Myocardial Uptake Characteristics of Hexakis (Alkylisonitrile) Technetium(I) Complexes Effect of Lipophilicity. *Invest. Radiol.* **1989**, *24*, 25−29.

(7) Abram, U.; Knop, G. Hexakis(isocyanoessigsäureethylester)-technetium(I) tetraphenylboranate, $[Tc(EEIN)_6]BPh_4$. *Z. Chem.* **1988**, *28*, 106−107.

(8) Kronauge, J. F.; Davison, A.; Roseberry, A. M.; Costello, C. E.; Maleknia, S.; Jones, A. G. Synthesis, and Identification of the Monocation $Tc(CPI)_6^+$ in $Tc(CNC(CH_3)_2COOCH_3)_6Cl$ and Its Hydrolysis Products. *Inorg. Chem.* **1991**, *30*, 4265−4271.

(9) Farr, J. P.; Abrams, M. J.; Costello, C. E.; Davison, A.; Lippard, S. J.; Jones, A. G. Higher coordinate complexes. Part 22. Synthesis and reactions of seven-coordinate technetium and rhenium alkyl isocyanide complexes. *Organometallics* **1985**, *4*, 139−142.

(10) Linder, K.; Davison, A.; Dewan, J. C.; Costello, C. E.; Maleknia, S. Nitrosyl Complexes of Technetium: Synthesis and Characterization of $[Tc^I(NO)(CNCMe_3)_5](PF_6)_2$ and $Tc(NO)Br_2(CNCMe_3)_3$ and the Crystal Structure of $Tc(NO)Br_2(CNCMe_3)_3$. *Inorg. Chem.* **1986**, *25*, 2085−2089.

(11) Abram, U.; Beyer, R.; Münze, R.; Findeisen, M. B.; Lorenz, B. Mixed-Ligand Complexes of Technetium. IV. Cationic, Hexacoordinated Tc(I) Complexes with Two Different Isocyanide Ligands in the Coordination Sphere, $[Tc(R^1NC)_k(R^2NC)_{6-k}]^+$ (k = 0 − 6). *Inorg. Chim. Acta* **1989**, *160*, 139−142.
(12) De Vries, N.; Davison, A.; Jones, A. G. Trigonal bipyramidal compounds of technetium with a tetradentate umbrella ligand. *Inorg. Chim. Acta* **1989**, *165*, 9−10.
(13) De Vries, N.; Cook, J.; Jones, A. G.; Davison, A. Technetium-(III) complexes with the tetradentate "umbrella" ligand tris(o-mercaptophenyl)phosphinate: x-ray structural characterization of $Tc(P(o\text{-}C_6H_4S)_3)(CNC_3H_7)$ and $Tc(P(o\text{-}C_6H_4S)_3)(CNC_3H_7)_2$. *Inorg. Chem.* **1991**, *30*, 2662−2665.
(14) Spies, H.; Glaser, M.; Pietzsch, H.-J.; Hahn, F. E.; Lügger, T. Synthesis and reactions of trigonal-bipyramidal, rhenium and technetium complexes with a tripodal, tetradentate NS3 ligand. *Inorg. Chim. Acta* **1995**, *240*, 465−478.
(15) Pietzsch, H.-J.; Gupta, A.; Syhre, R.; Leibnitz, P.; Spies, H. Mixed-Ligand Technetium(III) Complexes with Tetradendate/Monodendate NS_3/Isocyanide Coordination: A New Nonpolar Technetium Chelate System for the Design of Neutral and Lipophilic Complexes Stable *in Vivo*. *Bioconjugate Chem.* **2001**, *12*, 538−544.
(16) Spies, H.; Glaser, M.; Pietzsch, H.-J.; Hahn, F. E.; Kintzel, O.; Lügger, T. Trigonal-Bipyramidal Technetium and Rhenium Complexes with Tetradentate NS_3 Tripod Ligands. *Angew. Chem., Int. Ed. Engl.* **1994**, *33*, 1354−1356.
(17) Seifert, S.; Künstler, J. U.; Schiller, E.; Pietzsch, H.-J.; Pawelke, B.; Bergmann, R.; Spies, H. Novel Procedures for Preparing ^{99m}Tc-(III) Complexes with Tetradentate/Monodentate Coordination of Varying Lipophilicity and Adaptation to ^{188}Re Analogues. *Bioconjugate Chem.* **2004**, *15*, 856−863.
(18) Fernandes, C.; Santos, I. C.; Santos, I.; Pietzsch, H.-J.; Künstler, J.-U.; Kraus, W.; Rey, A.; Margaritis, N.; Bourkoula, A.; Chiotellis, A.; Paravatou-Petsotas, M.; Pirmettis, I. Rhenium and technetium complexes bearing quinazoline derivatives: progress towards a ^{99m}Tc biomarker for EGFR-TK imaging. *Dalton Trans.* **2008**, 3215−3225.
(19) Drews, A.; Pietzsch, H.-J.; Syhre, R.; Seifert, S.; Varnäs, K.; Hall, H.; Halldin, C.; Kraus, W.; Karlsson, P.; Johnsson, C.; Spies, H.; Johannsen, B. Synthesis and biological evaluation of technetium(III) mixed-ligand complexes with high affinity for the cerebral 5-HT1A receptor and the a1-adrenergic receptor. *Nucl. Med. Biol.* **2002**, *29*, 389−398.
(20) O'Connell, L. A.; Davison, A. Preparation and characterization of the complexes $[Tc(CN^tBu)_X(PPh_3)_{6-x}]PF_6$ (x=4, 5). *Inorg. Chim. Acta* **1990**, *176*, 7−9.
(21) Rochon, F. D.; Melanson, R.; Kong, Pi-C. Synthesis and crystal structure of mixed-ligand Tc (I) complexes, with dimethylphenylphosphine and t-butylisonitrile. *Inorg. Chim. Acta* **1996**, *245*, 251−256.
(22) Blanchard, S.; Nicholson, T.; Davison, A.; Jones, A. G. Ligand substitution reactions of $[Tc(NO)Cl_2(PPh_3)_2(NCCH_3)]$ with π-acceptor ligands. *Inorg. Chim. Acta* **1997**, *254*, 225−231.
(23) Abram, U.; Abram, S.; Beyer, R.; Münze, R.; Kaden, L.; Lorenz, B.; Findeisen, M. Mixed Ligand Complexes of Technetium. II. $[Tc(dppe)_2(R\text{-}NC)_2]^+$ Complexes (dppe = bis(diphenylphosphino)-ethane; R = tert. butyl, cyclohexyl). *Inorg. Chim. Acta* **1988**, *148*, 141−142.
(24) Kaden, L.; Pombeiro, A. J. L.; Wang, Y.; Abram, U. Mixed-ligand complexes of technetium. XIII. A new and facile synthesis, structure and electrochemical behaviour of *trans*-$[Tc(dppe)_2(bu^tNC)_2](PF_6)$ • ethanol (dppe = bis(diphenylphosphino)-ethane, bu^tNC = tert-butylisocyanide). *Inorg. Chim. Acta* **1995**, *230*, 189−192.
(25) Kaden, L.; Findeisen, M.; Lorenz, B.; Schmidt, K.; Wahren, M. $HTc(N_2)(dppe)_2$ as starting material for mixed-ligand complexes of technetium(I). *Inorg. Chim. Acta* **1992**, *193*, 213−215.
(26) O'Connell, L. A.; Dewan, J.; Jones, A. G.; Davison, A. Technetium(I) Isocyanide Complexes with Bidentate Aromatic Amine Ligands: Structural Characterization of $[Tc(CNtBu)_4(bpy)]$-PF_6, a Complex with "Tc(III) Character". *Inorg. Chem.* **1990**, *29*, 3539−3547.
(27) Nicholson, T.; Kramer, D. J.; Davison, A.; Jones, A. G. The substitution chemistry of a useful new synthon with neutral donor ligands. Part 2. The reactions of $[TcCl_3(N{=}NPh_2)(PPh_3)_2]$ with neutral nitrogen and carbon ligands. The X-ray structure of $[TcCl_2(N{=}NPh_2)(bipy)(PPh_3)][PF_6]$, $[TcCl_2(N{=}NPh_2)(terpy)]$-$[BF_4]$ and $[TcCl(N{=}NPh_2)(CNCH_2Ph)_2(PPh_3)_2][PF_6]$. *Inorg. Chim. Acta* **2003**, *353*, 269−275.
(28) Robinson, D. J.; Harris, G. W.; Boeyens, J. C. A.; Coville, N. J. A structural and kinetic investigation of the isomers of $M_2(CO)_8(CNBu^t)_2$ (M = Mn, Re). *J. Chem. Soc., Chem. Commun.* **1984**, 1307−1308.
(29) Harris, G. W.; Coville, N. J. The palladium(II) oxide-catalyzed reaction between decacarbonyldirhenium and isocyanides. *Organometallics* **1985**, *4*, 908−914.
(30) Miroslavov, A. E.; Lumpov, A. A.; Sidorenko, G. V.; Levitskaya, E. M.; Gorshkov, N. I.; Suglobov, D. N.; Alberto, R.; Braband, H.; Gurzhiy, V. V.; Krivovichev, S. V. I. G.; Tananaev, I. G. Complexes of technetium(I) (^{99}Tc, ^{99m}Tc) pentacarbonyl core with π-acceptor ligands (tert-butyl isocyanide and triphenylphosphine): Crystal structures of $[Tc(CO)_5(PPh_3)]OTf$ and $[Tc(CO)_5(CNC(CH_3)_3)]$-ClO_4. *J. Organomet. Chem.* **2008**, *693*, 4−10.
(31) Miroslavov, A. E.; Polotskii, Y. S.; Gurzhiy, V. V.; Ivanov, A. Yu.; Lumpov, A. A.; Tyupina, M. Yu.; Sidorenko, G. V.; Tolstoy, P. M.; Maltsev, D. A.; Suglobov, D. N. Technetium and Rhenium Pentacarbonyl Complexes with C_2 and C_{11} ω-Isocyanocarboxylic Acid Esters. *Inorg. Chem.* **2014**, *53*, 7861−7869.
(32) Hieber, W.; Lux, F.; Herget, C. Z. Über Kohlenoxidverbindungen des Technetiums. *Naturforsch* **1965**, *20*, 1159−1165.
(33) Lorenz, B.; Findeisen, M.; Olk, B.; Schmidt, K. Technetium(I) Complexes $Tc(CO)_3BrL_2$ (L = Phosphine, Pyridine, Isocyanide). *Z. Anorg. Allg. Chem.* **1988**, *566*, 160−168.
(34) Alberto, R.; Schibli, R.; Egli, A.; August Schubiger, W. A.; Herrmann, G.; Artus, U.; Abram, T. A.; Kaden, T. A. Metal carbonyl syntheses. XXII. Low-pressure carbonylation of $[MOCl_4]^-$ and $[MO_4]^-$. The technetium(I) and rhenium(l) complexes $[NEt_4]_2[MCl_3(CO)_3]$. *J. Organomet. Chem.* **1995**, *492*, 217−224.
(35) Alberto, R.; Schibli, R.; Angst, D.; Schubiger, P. A.; Abram, U.; Abram, S.; Kaden, T. A. Application of technetium and rhenium carbonyl chemistry to nuclear medicine. Preparation of $[NEt_4]_2[TcCl_3(CO)_3]$ from $[NBu_4][TcO_4]$ and structure of $[NEt_4]$-$[Tc_2(\mu\text{-}Cl)_3(CO)_6]$; structures of the model complexes $[NEt_4]$-$[Re_2(\mu\text{-}OEt)_2(\mu\text{-}OAc)(CO)_6]$ and $[ReBr(\{\text{-}CH_2S(CH_2)_2Cl\}_2)$-$(CO)_3]$. *Transition Met. Chem.* **1997**, *22*, 597−601.
(36) Hildebrand, S. $(NBu_4)[Tc_2(\mu\text{-}Cl)_3(CO)_6]$ als Startverbindung für Technetiumtricarbonylkomplexe. Ph.D. Thesis, Freie Universität Berlin, 2018.
(37) Alberto, R. R.; Schibli, A.; Egli, A. P.; Schubiger, A. P.; Abram, U.; Kaden, T. A. A Novel Organometallic Aqua Complex of Technetium for the Labeling of Biomolecules: Synthesis of $[^{99m}Tc(OH_2)_3(CO)_3]^+$ from $[^{99m}TcO_4]^-$ in Aqueous Solution and Its Reaction with a Bifunctional Ligand. *J. Am. Chem. Soc.* **1998**, *120*, 7987−7988.
(38) Mundwiler, S.; Kündig, M.; Ortner, K.; Alberto, R. A new [2 + 1] mixed ligand concept based on $[^{99(m)}Tc(OH_2)_3(CO)_3]^+$: a basic study. *Dalton Trans.* **2004**, 1320−1328.
(39) Gorshkov, N. I.; Lumpov, A. A.; Miroslavov, A. E.; Suglobov, D. N. 2+1 Chelating Systems for Binding Organometallic Fragment $Tc(CO)_3^+$. *Radiochemistry* **2005**, *47*, 45−49.
(40) Alberto, R.; Schibli, R.; August Schubiger, P. A.; Abram, U.; Kaden, T. A. Reactions with the technetium and rhenium carbonyl complexes $(NEt_4)_2[MX_3(CO)_3]$. Synthesis and structures of $[Tc(CN\text{-}Bu^t)_3(CO)_3](NO_3)$ and $(NEt_4)[Tc_2(\mu\text{-}SCH_2CH_2OH)_3(CO)_6]$. *Polyhedron* **1996**, *15*, 1079−1089.
(41) Claude, G.; Salsi, F.; Hagenbach, A.; Gembicky, M.; Neville, M.; Chan, C.; Figueroa, J. S.; Abram, U. Structural and Redox Variations in Technetium Complexes Supported by m-Terphenyl Isocyanides. *Organometallics* **2020**, *39*, 2287−2294.

https://doi.org/10.1021/acs.inorgchem.2c02730
Inorg. Chem. 2022, 61, 16163−16176

(42) Ditri, T.; Fox, B.; Moore, C.; Rheingold, A.; Figueroa, J. Effective Control of Ligation and Geometric Isomerism: Direct Comparison of Steric Properties Associated with Bis-mesityl and Bis-diisopropylphenyl m-Terphenyl Isocyanides. *Inorg. Chem.* **2009**, *48*, 8362−8375.
(43) Stewart, M. A.; Moore, C. E.; Ditri, T. B.; Labios, L. A.; Rheingold, A. L.; Figueroa, J. S. Electrophilic functionalization of well-behaved manganese monoanions supported by m-terphenyl isocyanides. *Chem. Commun.* **2011**, *47*, 406−408.
(44) Ditri, T. B.; Carpenter, A. E.; Ripatti, D. S.; Moore, C. E.; Rheingold, A. L.; Figueroa, J. S. Chloro- and Trifluoromethyl-Substituted Flanking-Ring m-Terphenyl Isocyanides: η_6-Arene Binding to Zero-Valent Molybdenum Centers and Comparison to Alkyl-Substituted Derivatives. *Inorg. Chem.* **2013**, *52*, 13216−13229.
(45) Salsi, F.; Neville, M.; Drance, M.; Hagenbach, A.; Chan, C. C.; Figueroa, J. S.; Abram, U. A closed-shell monomeric rhenium(1-) anion provided my m-terphenyl isocyanide ligation. *Chem. Commun.* **2020**, *56*, 7009−7012.
(46) Salsi, F.; Neville, M.; Drance, M.; Hagenbach, A.; Figueroa, J. S.; Abram, U. $\{M^{I}(CO)X(CNp\text{-}FAr^{DArF2})_4\}$ (DArF = 3,5-$(CF_3)_2C_6H_3$; M = Re, Tc; X = Br, Cl) Complexes: Convenient Platforms for the Synthesis of Low-valent Rhenium and Technetium Compounds. *Organometallics* **2021**, *40*, 1336−1343.
(47) Patil, P.; Ahmadian-Moghaddam, M.; Dömling, A. Isocyanide 2.0. *Green Chem.* **2020**, *22*, 6902−6911.
(48) Carpenter, A. E.; Mokhtarzadeh, C. C.; Ripatti, D. S.; Havrylyuk, I. R.; Kamezawa, C. E.; Moore, A. L.; Rheingold, J. S.; Figueroa, J. S. Comparative Measure of the Electronic Influence of Highly Substituted Aryl Isocyanides. *Inorg. Chem.* **2015**, *54*, 2936−2944.
(49) Sheldrick, G. M. *SADABS*; University of Göttingen: Germany, 1996.
(50) Coppens, P. *The Evaluation of Absorption and Extinction in Single-Crystal Structure Analysis. Crystallographic Computing*; Copenhagen, Muksgaard, 1979.
(51) Sheldrick, G. M. A short history of SHELX. *Acta Crystallogr.* **2008**, *64*, 112−122.
(52) Sheldrick, G. M. Crystal structure refinement with SHELXL. *Acta Crystallogr.* **2015**, *71*, 3−8.
(53) *Diamond—Crystal and Molecular Structure Visualization Crystal Impact*; Dr. H. Putz & Dr. K. Brandenburg GbR: Bonn, Germany, version 4.6.5, 2021.
(54) *High Performance Computing (HPC) System Curta at Freie Universität*: Berlin. DOI: 10.17169/refubium-26754.
(55) Frisch, M. J.; Trucks, G. W.; Schlegel, H. B.; Scuseria, G. E.; Robb, M. A.; Cheeseman, J. R.; Scalmani, G.; Barone, V.; Petersson, G. A.; Nakatsuji, H.; Li, X.; Caricato, M.; Marenich, A. V.; Bloino, J.; Janesko, B. G.; Gomperts, R.; Mennucci, B.; Hratchian, H. P.; Ortiz, J. V.; Izmaylov, A. F.; Sonnenberg, J. L.; Williams-Young, D.; Ding, F.; Lipparini, F.; Egidi, F.; Goings, J.; Peng, B.; Petrone, A.; Henderson, T.; Ranasinghe, D.; Zakrzewski, V. G.; Gao, J.; Rega, N.; Zheng, G.; Liang, W.; Hada, M.; Ehara, M.; Toyota, K.; Fukuda, R.; Hasegawa, J.; Ishida, M.; Nakajima, T.; Honda, Y.; Kitao, O.; Nakai, H.; Vreven, T.; Throssell, K.; Montgomery, J. A., Jr.; Peralta, J. E.; Ogliaro, F.; Bearpark, M. J.; Heyd, J. J.; Brothers, E. N.; Kudin, K. N.; Staroverov, V. N.; Keith, T. A.; Kobayashi, R.; Normand, J.; Raghavachari, K.; Rendell, A. P.; Burant, J. C.; Iyengar, S. S.; Tomasi, J.; Cossi, M.; Millam, J. M.; Klene, M.; Adamo, C.; Cammi, R.; Ochterski, J. W.; Martin, R. L.; Morokuma, K.; Farkas, O.; Foresman, J. B.; Fox, D. J. *Gaussian 16, Revision B.01*; Gaussian, Inc.: Wallingford CT, 2016.
(56) Dennington, R.; Keith, T. A.; Millam, J. M. *GaussView, Version 6*; Semichem Inc.: Shawnee Mission, KS, 2016.
(57) Hanwell, M. D.; Curtis, D. E.; Lonie, D. C.; Vandermeersch, C.; Zurek, E.; Hutchison, G. R. Avogadro: An advanced semantic chemical editor, visualization, and analysis platform. *J. Cheminf.* **2012**, *4*, 17.
(58) Vosko, S. H.; Wilk, L.; Nusair, M. Accurate spin-dependent electron liquid correlation energies for local spin density calculations: a critical analysis. *Can. J. Phys.* **1980**, *58*, 1200−1211.
(59) Becke, A. D. Density-functional thermochemistry. III. The role of exact exchange. *J. Chem. Phys.* **1993**, *98*, 5648−5652.
(60) Lee, C.; Yang, W.; Parr, R. G. Development of the Colle-Salvetti correlation-energy formula into a functional of the electron density. *Phys. Rev.* **1988**, *37*, 785−789.
(61) Curtiss, L. A.; McGrath, M. P.; Blaudeau, J.-P.; Davis, N. E.; Binning, R. C.; Radom, L. Extension of Gaussian-2 theory to molecules containing third-row atoms Ga-Kr. *J. Chem. Phys.* **1995**, *103*, 6104−6113.
(62) Glukhovtsev, M. N.; Pross, A.; McGrath, M. P.; Radom, L. Extension of Gaussian-2 (G2) theory to bromine- and iodine-containing molecules: Use of effective core potentials. *J. Chem. Phys.* **1995**, *103*, 1878−1885.
(63) Clark, T.; Chandrasekhar, J.; Spitznagel, G. W.; Schleyer, P. V. R. Efficient diffuse function-augmented basis sets for anion calculations. III. The 3-21+G basis set for first-row elements, Li-F. *J. Comput. Chem.* **1983**, *4*, 294−301.
(64) Francl, M. M.; Pietro, W. J.; Hehre, W. J.; Binkley, J. S.; Gordon, M. S.; DeFrees, D. J.; Pople, J. A. Self-consistent molecular orbital methods. XXIII. A polarization-type basis set for second-row elements. *J. Chem. Phys.* **1982**, *77*, 3654−3665.
(65) Krishnan, R.; Binkley, J. S.; Seeger, R.; Pople, J. A. Self-consistent molecular orbital methods. XX. A basis set for correlated wave functions. *J. Chem. Phys.* **1980**, *72*, 650−654.
(66) McLean, A. D.; Chandler, G. S. Contracted Gaussian basis sets for molecular calculations. I. Second row atoms, Z=11-18. *J. Chem. Phys.* **1980**, *72*, 5639−5648.
(67) Spitznagel, G. W.; Clark, T.; von Ragué Schleyer, P.; Hehre, W. J. An evaluation of the performance of diffuse function-augmented basis sets for second row elements, Na-Cl. *J. Comput. Chem.* **1987**, *8*, 1109−1116.
(68) Schuchardt, K. L.; Didier, B. T.; Elsethagen, T.; Sun, L.; Gurumoorthi, V.; Chase, J.; Li, J.; Windus, T. L. Basis Set Exchange: A Community Database for Computational Sciences. *J. Chem. Inf. Model.* **2007**, *47*, 1045−1052.
(69) Lu, T.; Chen, F. Multiwfn: A multifunctional wavefunction analyzer. *J. Comput. Chem.* **2012**, *33*, 580−592.
(70) Mikhalev, V. A. ^{99}Tc NMR Spectroscopy. *Radiochemistry* **2005**, *47*, 319−333.
(71) Malatesta, L.; Bonati, F. *Isocyanide Complexes of Metals*; Wiley: London, 1969.
(72) Treichel, P. M. Transition Metal-Isocyanide Complexes. *Adv. Organomet. Chem.* **1973**, *11*, 21−86.
(73) Singleton, E.; Oosthuizen, H. E. Metal Isocyanide Complexes. *Adv. Organomet. Chem.* **1983**, *22*, 209−310.
(74) Weber, L. Homoleptic Isocyanide metallates. *Angew. Chem., Int. Ed. Engl.* **1998**, *37*, 1515−1517.
(75) Hieber, W. Über Metallisonitrile. *Z. Naturforsch.* **1950**, *5*, 129−130.
(76) Klages, F.; Mönkemeyer, K. I. Über Isonitrilkomplexe, I. Mitteil.: Darstellung und Eigenschaften aromatischer Nickeltetraisonitrile. Ein chemisches Argument für die Nitrilstruktur der Blausäure (vorläufige Mitteilung). *Chem. Ber.* **1950**, *83*, 501−508.
(77) Treichel, P. M.; Williams, J. P. Rhenium(I) isocyanide complexes. *J. Organomet. Chem.* **1977**, *135*, 39−51.
(78) Kottelat, E.; Chabert, V.; Crochet, A.; Fromm, K. M.; Zobi, F. Towards Cardiolite-Inspired Carbon Monoxide Releasing Molecules − Reactivity of d^4, d^5 Rhenium and d^6 Manganese Carbonyl Complexes with Isocyanide Ligands. *Eur. J. Inorg. Chem.* **2015**, *2015*, 5628−5638.
(79) Cheung, A. W.; Lo, L. T.-S.; Ko, C.-C.; Yiu, S.-M. Synthesis, Functionalization, Characterization, and Photophysical Study of Carbonyl-Containing Isocyano Rhenium(I) Diimine Complexes. *Inorg. Chem.* **2011**, *50*, 4798−4810.
(80) Kuty, D. W.; Alexander, J. J. Reactions of Isocyanides with Alkylpentacarbonylmanganese. *Inorg. Chem.* **1978**, *17*, 1489−1494.
(81) Halbauer, K.; Görls, H.; Fidler, T.; Imhof, J. The reaction of manganese carbonyl with tert-butylisocyanide: Synthesis and

https://doi.org/10.1021/acs.inorgchem.2c02730
Inorg. Chem. 2022, 61, 16163−16176

characterization of *cis*- and *trans*-[$Mn^{I}(^{t}BuNC)_4(CN)(CO)$]. *Organomet. Chem.* **2007**, *692*, 1898−1911.
(82) Carl, K.; Sterzik, A.; Görls, H.; Imhof, W. Synthesis of Trinuclear Heterobimetallic Cyanido-Bridged Complexes from the Reaction of [$Mn^{I}(CN)(CO)(^{t}BuNC)_4$] with Transition-Metal Chlorides. *Eur. J. Inorg. Chem.* **2014**, *2014*, 4349−4356.
(83) Agnew, D. W.; Sampson, M. D.; Moore, C. E.; Rheingold, A. L.; Kubiak, C. P.; Figueroa, J. S. Electrochemical Properties and CO_2-Reduction Ability of m-Terphenyl Isocyanide Supported Manganese Tricarbonyl Complexes. *Inorg. Chem.* **2016**, *55*, 12400−12408.
(84) Kuznetsov, M. L. Theoretical studies of transition metal complexes with nitriles and isocyanides. *Russ. Chem. Rev.* **2002**, *71*, 265−282.
(85) Csonka, I. P.; Szepes, L.; Modelli, A. Donor−acceptor properties of isonitriles studied by photoelectron spectroscopy and electron transmission spectroscopy. *J. Mass Spectrom.* **2004**, *39*, 1456−1466.
(86) Saillard, J. Y.; Le Beuze, A.; Simonneaux, G.; Le Maux, P.; Jaouen, G. Variation of R in the isocyanide series RNC: as an example of the concept of controlled modifications of the properties of ligands for organometallic synthesis. *J. Mol. Struct.* **1981**, *86*, 149−154.
(87) Guy, M. P.; Guy, J. T., Jr.; Bennett, D. W. A theoretical comparison of the electronic structures of alkyl and aryl isocyanide ligands. *J. Mol. Struct.* **1985**, *122*, 95−99.
(88) Tasi, G.; Pálinkó, I. Using Molecular Electrostatic Potential Maps for Similarity Studies. *Topics in Current Chemistry*; Springer, 1995, Vol. *174*, pp 46−71.
(89) Kikuchi, O.; Yamaguchi, K.; Morihashi, K.; Yokoyama, Y.; Nakayama, M. Molecular Eltrostatic Potential Map Analysis of Metal Cation Interaction with Nucleophilic Molecules. *Bull. Chem. Soc. Jpn.* **1993**, *66*, 2412−2414.
(90) Lu, T.; Chen, F. Quantitative analysis of molecular surface based on improved Marching Tetrahedra algorithm. *J. Mol. Graphics Modell.* **2012**, *38*, 314−323.
(91) Lentz, D.; Graske, K.; Preugschat, D. Synthesis of Pentafluorophenyl Isocyanide and Its Stabilization as a Ligands in $Cp^*Mn(CO)_2(CN\text{-}C_6F_5)$. *Chem. Ber.* **1988**, *121*, 1445−1447.
(92) Noll, B.; Leibnitz, P.; Spies, H. *Cambridge Structural Data Base*, Entry AMUCAM.
(93) Tulip, T. H.; Calabrese, J.; Kronauge, J. F.; Davison, A.; Jones, A. G.; *Technetium in Chemistry and Nuclear Medicine*; Nicolini, M.; Bandoli, G.; Mazzi, U., Eds.; Cortina International: Verona, 1986, p 119.
(94) O'Connell, L. A.; Pearlstein, R. M.; Davison, A.; Thornback, J. R.; Kronauge, J. F.; Jones, A. G. Technetium-99 NMR spectroscopy: chemical shift trends and long range coupling effects. *Inorg. Chim. Acta* **1989**, *161*, 39−43.
(95) Mizuno, Y.; Uehara, T.; Hanaoka, H.; Endo, Y.; Jen, C.-W.; Arano, Y. Purification-Free Method for Preparing Technetium-99m-Labeled Multivalent Probes for Enhanced *in Vivo* Imaging of Saturable Systems. *J. Med. Chem.* **2016**, *59*, 3331−3339.
(96) Mizuno, Y.; Uehara, T.; Jen, C.-W.; Akizawa, H.; Arano, Y. The synthesis of a ^{99m}Tc-labeled tetravalent targeting probe upon isonitrile coordination to $^{99m}Tc^{I}$ for enhanced target uptake in saturable systems. *RSC Adv.* **2019**, *9*, 26126−26135.
(97) Mizuno, Y.; Komatsu, N.; Uehara, T.; Shimoda, Y.; Kimura, K.; Arano, Y.; Akizawa, H. Aryl isocyanide derivative for one-pot synthesis of purification-free ^{99m}Tc-labeled hexavalent targeting probe. *Nucl. Med. Biol.* **2020**, *86*−*87*, 30−36.

https://doi.org/10.1021/acs.inorgchem.2c02730
Inorg. Chem. 2022, 61, 16163−16176